

Next to SV resummed prediction for pseudoscalar higgs boson production at NNLO+NNLL

Arunima Bhattacharya,^{1,*} M. C. Kumar,^{2,†} Prakash Mathews,^{1,‡} and V. Ravindran^{3,§}

¹*Saha Institute of Nuclear Physics, HBNI, 1/AF Saltlake, Kolkata 700064, India*

²*Department of Physics, Indian Institute of Technology Guwahati, Guwahati-781039, Assam, India*

³*The Institute of Mathematical Sciences, HBNI, Taramani, Chennai-600113, India*

We present first results on the resummation of Next-to-Soft Virtual (NSV) logarithms for the threshold production of pseudoscalar higgs boson through gluon fusion at the LHC. These results are presented after resumming the NSV logarithms of the kind $\log^i(1-z)$ to NNLL accuracy and match them systematically to the fixed order NNLO cross-sections. These results are obtained using collinear factorization, renormalization group invariance and recent developments in NSV resummation techniques. The phenomenological implications of these NSV resummed results for 13 TeV LHC are studied and it is observed that these NSV logarithms are quite large. We also study theory uncertainties and find that the renormalization scale uncertainties get reduced further with the inclusion of NSV corrections at various orders in QCD.

I. INTRODUCTION

The ATLAS [1] and CMS [2] collaborations of the Large Hadron Collider (LHC) have been successful in discovering the Higgs boson of the standard model (SM) and this has put the SM on a very strong footing. As a result, a lot of work has been going on to investigate the properties and interactions of this discovered Higgs boson with the other SM particles [3–11]. Despite this phenomenal success, it is widely known that the SM fails to explain certain natural phenomena such as the baryon asymmetry in the universe, existence of dark matter, tiny non-zero mass of neutrinos, etc. In order to explain these phenomena, one has to go beyond the realm of the SM. Supersymmetric theories provide one such solution to the above mentioned problems. The minimal supersymmetric extension of the SM (MSSM) is one of the simplest forms of the supersymmetric theories. It has five Higgs bosons, out of which two are neutral scalars (h,H), one is a pseudoscalar (A) and the remaining two are charged scalars (H^\pm). The pseudoscalar Higgs boson which is CP odd could be as light as the discovered Higgs boson. Hence, a dedicated effort has been going on to determine the CP property of the discovered Higgs boson, and to identify it with that of the SM, although there are already indications that it is a scalar with even parity [10, 11]. This necessitates the requirement of precise predictions for relevant observables of both scalar and pseudoscalar ones.

Higher order corrections in perturbative QCD (pQCD) provide a way to achieve the required precision. The pseudoscalar production cross-sections are available to NNLO accuracy in QCD [12–14]. The corrections are large and are of the order of 67% at NLO and get increased by an additional 15% at the NNLO level for the renormalization and factorization scales set to $\mu_R = \mu_F = m_A/2$ for the pseudoscalar mass $m_A = 200$ GeV. The large size of these corrections imply that in order to achieve precise theoretical results, corrections of even higher orders are necessary.

The pseudoscalar Higgs production takes place in gluon fusion channel via quark loop and the LO results for finite quark mass (exact) dependence are already available. The calculation becomes simpler in the infinite quark mass limit (Effective Field Theory) and this makes it easy to compute cross-sections at higher orders in perturbation theory. This effective field theory (EFT) approach in the case of scalar Higgs boson production [14–16] became extremely successful as the difference between the exact and EFT results at NNLO level were found to be within 1% [17–19]. For pseudoscalar production at the hadron colliders, NNLO predictions are already available [13, 14, 20].

In [21, 22] the computation of complete N³LO predictions for the scalar Higgs boson production through gluon fusion at the hadron colliders in the effective theory has been accomplished. These third order corrections increase the cross-section by about 3.1% for the central scale choice of $m_H/2$ while the corresponding scale uncertainty has reduced to as small as below 2%. In a recent study for neutral current Drell-Yan process [23], the complete N³LO results have been calculated for the first time. The corresponding cross-section is found to be about 0.992 times that of the NNLO cross-section for the invariant mass region $Q = 300$ GeV indicating a small negative correction from the third order in this kinematic region. The scale uncertainty at N³LO level is found to be very mild, however, it has been observed that the scale uncertainty bands for N³LO and NNLO level cross-sections do not overlap with

* arunima.bhattacharya@saha.ac.in

† mckumar@iitg.ac.in

‡ prakash.mathews@saha.ac.in

§ ravindra@imsc.res.in

each other. The next step in the process is the computation of N³LO cross-sections for the pseudoscalar production through gluon fusion. The first task in this direction is to obtain the threshold enhanced cross-section at N³LO level and the same has already been computed in [24]. Further, the approximate full N³LO_A results are also available for the pseudoscalar Higgs boson case [25].

However, these fixed order (FO) QCD predictions have limited applicability because of the presence of large logarithmic contributions that arise in the threshold region of pseudoscalar production. At the threshold, the emission of soft gluons gives large logarithmic contributions to the cross-section when the partonic center of mass energy approaches the pseudoscalar mass m_A . If these large logarithms arising from the soft gluons can be resummed to all orders in perturbation theory, then the problem of spoiling the reliability of FO perturbative predictions can be solved. We denote the SV resummed results by LL, NLL, etc. The next-to-next-to-leading logarithmic (NNLL) resummed results [26–34] give a sizable contribution and reduce scale uncertainties. These logarithms in the parton level cross-section $d\hat{\sigma}$ computed to order α_s^k will appear as

$$\alpha_s^k \left[\frac{\ln^i(1-z)}{1-z} \right]_+, \text{ where } i < 2k - 1. \quad (1)$$

Here, the subscript $+$ denotes the plus function and $z = m_A^2/s$ with $z \rightarrow 1$ limit representing the parton threshold region. The precise contribution of these parton level logarithms to the hadron level cross-section depends on the corresponding parton fluxes in that region. For the case of Higgs mass region (125 GeV), the associated gluon flux is large and hence these threshold logarithms due to the soft and collinear gluons are also found to be significant. This way of resumming a set of large logarithms and then matching them to the FO results can give robust theoretical predictions.

For the scalar Higgs boson production, the FO results are available at N³LO level [22, 35] and the corresponding threshold resummed results have been computed to N³LL accuracy [36, 37]. The computation of the three loop threshold corrections for pseudoscalar higgs boson production in the threshold limit has been done in [38]. A knowledge of the form factors up to three loop level is needed to calculate the threshold corrections to pseudoscalar production at N³LO level.

Further, the UV and IR divergences give rise to most of the logarithms at higher orders in the intermediate stages of the computations. These logarithms depend on the renormalization and factorization scales and are present in the perturbative expansions. Such logarithms help to estimate the error in theory predictions resulting from the truncation of the perturbation theory to a finite order.

There are various studies on the computation of SV results in QCD corresponding to a number of observable produced in hadron collisions. For SV results up to third order, see [29, 30, 39–45]. A series of works in this direction have been carried out for the resummation of the threshold logarithms following the path breaking works by Sterman *et al.* [46] and Catani *et al.* [47]. See [37, 48–52] for Higgs production in gluon fusion, [53, 54] for bottom quark annihilation and for Drell-Yan (DY) [42, 49, 55–57]. In z -space, one has to deal with convolutions of these distributions and so, one moves to the Mellin space approach which uses the conjugate variable N for resummation. The distributions $\mathcal{D}_i(z)$ become functions of $\log^{i+1}(N)$ where we suppress terms of $\mathcal{O}(1/N)$ in the threshold limit of $N \rightarrow \infty$.

However, it has also been observed that at higher orders in QCD threshold corrections alone can not replace the full FO results and in fact it is found that the role of the NSV terms namely $\log^i(1-z)$, $i = 0, 1, \dots$ are also important. These NSV contributions can, in principle, originate from parton channels other than the one that corresponds to Born contribution. It will also be important to see whether these NSV terms can be resummed systematically to all orders exactly like the leading SV terms. Several advancements in this direction have been made [58–68]. In [69], theories of mass factorization, renormalization group invariance and Sudakov K-plus-G equation have been exploited to provide a result in z - and N -space to predict NSV terms for DY and Higgs boson production to all orders in perturbation theory. In [70], the NSV resummation has been achieved to Leading Logarithmic (LL) accuracy for color singlet production processes in hadron collisions. It has been observed that the resummation of NSV logarithms in the diagonal channel gives large contributions to the cross-sections, while those from the qg channel are found to give negative contribution of about 3% in the high mass region. It has also been noticed that the inclusion of NSV resummed results increases scale uncertainties obtained from the SV resummation.

In this article, we compute the NSV corrections for the pseudoscalar higgs boson production process at N³LO level based on the formalism developed in [29, 69, 71] and the recent result at this order for scalar production [22]. We also further study the phenomenological impact of resumming these NSV logarithms to NNLL accuracy after they are systematically matched to the FO NNLO ones. We represent the resummed results for the production of pseudoscalar higgs boson at leading logarithmic, next-to leading logarithmic and next-to-next-to leading logarithmic accuracy by LL, NLL and NNLL when we take into account both SV and NSV threshold logarithms. The Section II is devoted to developing the theoretical basis for this work. The Section III deals with the threshold corrections to the

cross-section - the several ingredients required and subsequently, a detailed explanation of these elements. In Section IV, we present the analytical results for resumming the NSV logarithms to NLL accuracy. In Section V we recollect the NSV resummation formalism developed recently in [69] and in Section VI we present the numerical results for the production of pseudoscalar Higgs boson for 13 TeV LHC. Then we conclude this article.

II. THEORETICAL FRAMEWORK

Coupling of a pseudoscalar higgs boson to gluons happens through a virtual heavy top quark loop indirectly which can be integrated out in the infinite top quark mass limit. The effective lagrangian [72] that is used to describe the interaction of the pseudoscalar fields $\Phi^A(x)$ with gauge fields *via* the pseudoscalar gluonic operators $O_G(x)$, and with light quark fields *via* the pseudoscalar fermionic operator $O_J(x)$ are given by

$$\mathcal{L}_{eff}^A = \Phi^A(x) \left[-\frac{1}{8} C_G O_G(x) - \frac{1}{2} C_J O_J(x) \right]. \quad (2)$$

The pseudoscalar gluonic and fermionic operators are defined as

$$O_G(x) = G^{a\mu\nu} \tilde{G}_{\mu\nu}^a = \epsilon_{\mu\nu\rho\sigma} G^{a\mu\nu} G^{a\rho\sigma}, \quad G^{a\mu\nu} = \partial^\mu G^{a\nu} - \partial^\nu G^{a\mu} + g f^{abc} G_b^\mu G_c^\nu, \quad (3)$$

$$O_J(x) = \partial_\mu (\bar{\psi} \gamma^\mu \gamma^5 \psi), \quad (4)$$

where $G_{\mu\nu}^a$ is the gluonic field strength tensor and $\epsilon_{\mu\nu\rho\sigma}$ is the Levi-Civita tensor. The pseudoscalar fermionic operator $O_J(x)$ is the derivative of the singlet axial vector current. The light quark field and its conjugate are represented by ψ and $\bar{\psi}$ respectively. As we integrate out the heavy top quark degrees of freedom, the Wilson coefficients C_G and C_J show a dependence on the mass of the top quark m_t . As a result of the Adler-Bardeen theorem [73], there is no QCD corrections to C_G beyond one-loop. On the other hand, C_J begins only at second-order in the strong coupling constant. These coefficients are expanded in powers of the renormalized strong coupling constant as a series of $a_s \equiv g_s^2/16\pi^2 = \alpha_s/4\pi$. The Wilson coefficients are given by

$$C_G(a_s) = -a_s 2^{\frac{5}{4}} G_F^{\frac{1}{2}} \cot \beta, \quad (5)$$

$$C_J(a_s) = - \left[a_s C_F \left(\frac{3}{2} - 3 \ln \frac{\mu_R^2}{m_t^2} \right) + a_s^2 C_J^{(2)} + \dots \right] C_G, \quad (6)$$

where G_F is the Fermi constant, $\cot \beta$ is the ratio of the two Higgs doublets' vacuum expectation values in a generic two-Higgs doublet model, C_F is the quadratic Casimir in the fundamental representation of QCD and μ_R is the renormalization scale at which a_s is renormalized.

The unrenormalized strong coupling constant \hat{a}_s is related to renormalized one a_s by

$$\hat{a}_s S_\varepsilon = \left(\frac{\mu^2}{\mu_R^2} \right)^{\varepsilon/2} Z_{a_s} a_s, \quad (7)$$

with

$$S_\varepsilon = \exp[(\gamma_E - \ln 4\pi)\varepsilon/2],$$

where the renormalization constant Z_{a_s} up to order a_s^3 is given by [38, 71, 74]

$$Z_{a_s} = 1 + a_s \left[\frac{2}{\epsilon} \beta_0 \right] + a_s^2 \left[\frac{4}{\epsilon^2} \beta_0^2 + \frac{1}{\epsilon} \beta_1 \right] + a_s^3 \left[\frac{8}{\epsilon^3} \beta_0^3 + \frac{14}{3\epsilon^2} \beta_0 \beta_1 + \frac{2}{3\epsilon} \beta_2 \right]. \quad (8)$$

Here μ is the scale introduced to keep the strong coupling constant dimensionless in $d = 4 + \varepsilon$ space-time dimensions. The QCD β functions (β_i) have the standard definitions [74].

III. THRESHOLD CORRECTIONS

The inclusive cross-section for a pseudoscalar higgs boson production at the hadron colliders can be computed using [24]

$$\sigma^A(\tau, m_A^2) = \sigma^{A,(0)}(\mu_R^2) \sum_{a,b=q,\bar{q},g} \int_\tau^1 dy \Phi_{ab}(y, \mu_F^2) \Delta_{ab}^A\left(\frac{\tau}{y}, m_A^2, \mu_R^2, \mu_F^2\right), \quad (9)$$

where $\sigma^{A,(0)}(\mu_R^2)$ is the born cross-section at the parton level with finite top mass dependence and is given by

$$\sigma^{A,(0)}(\mu_R^2) = \frac{\pi\sqrt{2}G_F}{16} a_s^2 \cot^2 \beta |\tau_A f(\tau_A)|^2. \quad (10)$$

In the above equation, $\tau_A = 4m_t^2/m_A^2$ and the function $f(\tau_A)$ is given by

$$f(\tau_A) = \begin{cases} \arcsin^2 \frac{1}{\sqrt{\tau_A}} & \tau_A \geq 1 \\ -\frac{1}{4} \left(\ln \frac{1-\sqrt{1-\tau_A}}{1+\sqrt{1-\tau_A}} + i\pi \right)^2 & \tau_A < 1 \end{cases} \quad (11)$$

The parton flux is given by

$$\Phi_{ab}(y, \mu_F^2) = \int_y^1 \frac{dx}{x} f_a(x, \mu_F^2) f_b\left(\frac{y}{x}, \mu_F^2\right), \quad (12)$$

where f_a and f_b are the parton distribution functions (PDFs) of the initial state partons a and b , renormalized at the factorization scale μ_F . Here, $\Delta_{ab}^A(\tau/y, m_A^2, \mu_R^2, \mu_F^2)$ represent the parton level cross-section for the sub-process initiated by the a and b partons. This is the final result obtained after performing the UV renormalization at scale μ_R and the mass factorization at scale μ_F .

The chief aim of this article is to study how the contribution from soft gluons affects the cross-section for pseudoscalar production at hadron colliders. We get the final result that is infrared (IR) safe by adding the soft part of the cross-section to the ultraviolet (UV) renormalized virtual part. However, even this is not enough as mass factorization is needed to be done using appropriate counter terms. This combination is what is known as the soft-plus-virtual (SV) cross-section and the remaining part is known as the hard part. While the resummed results provide reliable predictions that can be compared against the experimental data, it is important to find out the role of sub-leading terms namely $\log^i(1-z)$, $i = 0, 1, \dots$. We call them NSV contributions. Thus, we write the partonic cross-section as

$$\Delta_{gg}^A(z, q^2, \mu_R^2, \mu_F^2) = \Delta_{gg}^{A,NSV}(z, q^2, \mu_R^2, \mu_F^2) + \Delta_{gg}^{A,hard}(z, q^2, \mu_R^2, \mu_F^2), \quad (13)$$

with $z \equiv q^2/\hat{s} = \tau/(x_1 x_2)$. Here $\Delta_{gg}^{A,NSV}(z, q^2, \mu_R^2, \mu_F^2)$ includes the threshold SV contributions, $\Delta_{gg}^{A,SV}(z, q^2, \mu_R^2, \mu_F^2)$, that contains distributions of type $\delta(1-z)$ and \mathcal{D}_i where the latter is defined as

$$\mathcal{D}_i \equiv \left[\frac{\ln^i(1-z)}{1-z} \right]_+. \quad (14)$$

On the contrary, the hard part of the cross-section, $\Delta_{gg}^{A,hard}(z, q^2, \mu_R^2, \mu_F^2)$, contains all regular terms in z .

The NSV cross-section in z -space is computed in $d = 4 + \varepsilon$ dimensions using [69]

$$\Delta_{gg}^{A,NSV}(z, q^2, \mu_R^2, \mu_F^2) = \mathcal{C} \exp \{ \Psi_g^A(z, q^2, \mu_R^2, \mu_F^2, \varepsilon) \} |_{\varepsilon=0} \quad (15)$$

where $\Psi_g^A(z, q^2, \mu_R^2, \mu_F^2, \varepsilon)$ is a finite distribution and \mathcal{C} is the convolution defined as

$$\mathcal{C}e^{f(z)} = \delta(1-z) + \frac{1}{1!}f(z) + \frac{1}{2!}f(z) \otimes f(z) + \dots \quad (16)$$

Here \otimes represents convolution and $f(z)$ is a distribution of the kind $\delta(1-z)$ and \mathcal{D}_i . The subscript g signifies the gluon initiated production of the pseudoscalar Higgs boson. An equivalent formalism can be done in the Mellin (N -moment) space, which replaces the distributions in z by continuous functions of the variable N . In this space, the threshold limit of $z \rightarrow 1$ changes to $N \rightarrow \infty$. The finite distribution Ψ_g^A depends on the form factors $\mathcal{F}_g^A(\hat{a}_s, Q^2, \mu^2, \varepsilon)$ with $Q^2 = -q^2$, the overall operator UV renormalization constant $Z_g^A(\hat{a}_s, \mu_R^2, \mu^2, \varepsilon)$, the soft collinear distribution $\Phi_g(\hat{a}_s, q^2, \mu^2, z, \varepsilon)$ and the mass factorization kernels $\Gamma_{gg}(\hat{a}_s, \mu_F^2, \mu^2, z, \varepsilon)$. The $\Psi_g^A(z, q^2, \mu_R^2, \mu_F^2, \varepsilon)$ can be written in terms of these quantities in the following form as [24]

$$\begin{aligned} \Psi_g^A(z, q^2, \mu_R^2, \mu_F^2, \varepsilon) = & \left(\ln [Z_g^A(\hat{a}_s, \mu_R^2, \mu^2, \varepsilon)]^2 + \ln |\mathcal{F}_g^A(\hat{a}_s, Q^2, \mu^2, \varepsilon)| \right) \delta(1-z) \\ & + 2\Phi_g(\hat{a}_s, q^2, \mu^2, z, \varepsilon) - 2\mathcal{C} \ln \Gamma_{gg}(\hat{a}_s, \mu_F^2, \mu^2, z, \varepsilon). \end{aligned} \quad (17)$$

In the next few sections, we will elaborate on how to get these ingredients to compute the NSV cross-section for pseudoscalar production at N³LO in gluon fusion.

A. Operator Renormalization Constant

After the strong coupling constant renormalization through Z_{a_s} , the form factor $\mathcal{F}_g^A(\hat{a}_s, Q^2, \mu^2, \varepsilon)$ still does not become completely UV finite. The additional renormalization required to remove the residual UV divergences is called the overall operator renormalization and is done using the constant Z_g^A . This is determined by solving the underlying RG equation [24]:

$$\mu_R^2 \frac{d}{d\mu_R^2} \ln Z_g^A(\hat{a}_s, \mu_R^2, \mu^2, \varepsilon) = \sum_{i=1}^{\infty} a_s^i \gamma_{g,i}^A, \quad (18)$$

where the UV anomalous dimensions $(\gamma_{g,i}^A)$ upto three-loop ($i = 3$) are obtained as following:

$$\gamma_{g,1}^A = \beta_1, \quad (19)$$

$$\gamma_{g,2}^A = \beta_2, \quad (20)$$

$$\gamma_{g,3}^A = \beta_3. \quad (21)$$

Using the above RG equation and the solutions of $\gamma_{g,i}^A$'s, we obtain the overall renormalization constant up to three-loop level:

$$\begin{aligned} Z_g^A = & 1 + a_s \left[\frac{22}{3\varepsilon} C_A - \frac{4}{3\varepsilon} n_f \right] \\ & + a_s^2 \left[\frac{1}{\varepsilon^2} \left\{ \frac{484}{9} C_A^2 - \frac{176}{9} C_A n_f + \frac{16}{9} n_f^2 \right\} + \frac{1}{\varepsilon} \left\{ \frac{34}{3} C_A^2 - \frac{10}{3} C_A n_f - 2 C_F n_f \right\} \right] \\ & + a_s^3 \left[\frac{1}{\varepsilon^3} \left\{ \frac{10648}{27} C_A^3 - \frac{1936}{9} C_A^2 n_f + \frac{352}{9} C_A n_f^2 - \frac{64}{27} n_f^3 \right\} \right. \\ & + \frac{1}{\varepsilon^2} \left\{ \frac{5236}{27} C_A^3 - \frac{2492}{27} C_A^2 n_f - \frac{308}{9} C_A C_F n_f + \frac{280}{27} C_A n_f^2 + \frac{56}{9} C_F n_f^2 \right\} \\ & \left. + \frac{1}{\varepsilon} \left\{ \frac{2857}{81} C_A^3 - \frac{1415}{81} C_A^2 n_f - \frac{205}{27} C_A C_F n_f + \frac{2}{3} C_F^2 n_f + \frac{79}{81} C_A n_f^2 + \frac{22}{27} C_F n_f^2 \right\} \right]. \quad (22) \end{aligned}$$

As can be seen, $Z_g^A = Z_{GG}$ where Z_{GG} is the renormalization constant for O_G operators which have been discussed in detail in [38, 75].

B. The Form Factor

The unrenormalized form factor, $\hat{\mathcal{F}}_g^{A,(n)}$, can be expanded in terms of \hat{a}_s as below:

$$\mathcal{F}_g^A \equiv \sum_{n=0}^{\infty} \left[\hat{a}_s^n \left(\frac{Q^2}{\mu^2} \right)^{n\frac{\varepsilon}{2}} S_\varepsilon^n \hat{\mathcal{F}}_g^{A,(n)} \right]. \quad (23)$$

The unrenormalized results for the choice of the scale $\mu_R^2 = \mu_F^2 = q^2$ are given up to two loop in [76] and up to three loop in [24]. These are required in the context of computing NSV cross-section as discussed below. The fact that QCD amplitudes obey factorization property, gauge and renormalization group (RG) invariances lead to the consequence that the form factor $\mathcal{F}_g^A(\hat{a}_s, Q^2, \mu^2, \varepsilon)$ satisfies the following K+G type differential equation [24, 77–81]:

$$Q^2 \frac{d}{dQ^2} \ln \mathcal{F}_g^A(\hat{a}_s, Q^2, \mu^2, \varepsilon) = \frac{1}{2} \left[K_g^A \left(\hat{a}_s, \frac{\mu_R^2}{\mu^2}, \varepsilon \right) + G_g^A \left(\hat{a}_s, \frac{Q^2}{\mu_R^2}, \frac{\mu_R^2}{\mu^2}, \varepsilon \right) \right]. \quad (24)$$

All the poles in ε are contained in the Q^2 independent function K_g^A and those which are finite as $\varepsilon \rightarrow 0$ are contained in G_g^A . The solution of the above K+G equation is given in a desirable form as below [82]:

$$\ln \mathcal{F}_g^A(\hat{a}_s, Q^2, \mu^2, \varepsilon) = \sum_{i=1}^{\infty} \hat{a}_s^i \left(\frac{Q^2}{\mu^2} \right)^{i\frac{\varepsilon}{2}} S_\varepsilon^i \hat{\mathcal{L}}_{g,i}^A(\varepsilon), \quad (25)$$

with

$$\hat{\mathcal{L}}_{g,1}^A(\varepsilon) = \frac{1}{\varepsilon^2} \{-2A_{g,1}^A\} + \frac{1}{\varepsilon} \{G_{g,1}^A(\varepsilon)\}, \quad (26)$$

$$\hat{\mathcal{L}}_{g,2}^A(\varepsilon) = \frac{1}{\varepsilon^3} \{\beta_0 A_{g,1}^A\} + \frac{1}{\varepsilon^2} \left\{ -\frac{1}{2} A_{g,2}^A - \beta_0 G_{g,1}^A(\varepsilon) \right\} + \frac{1}{\varepsilon} \left\{ \frac{1}{2} G_{g,2}^A(\varepsilon) \right\}, \quad (27)$$

$$\begin{aligned} \hat{\mathcal{L}}_{g,3}^A(\varepsilon) = & \frac{1}{\varepsilon^4} \left\{ -\frac{8}{9} \beta_0^2 A_{g,1}^A \right\} + \frac{1}{\varepsilon^3} \left\{ \frac{2}{9} \beta_1 A_{g,1}^A + \frac{8}{9} \beta_0 A_{g,2}^A + \frac{4}{3} \beta_0^2 G_{g,1}^A(\varepsilon) \right\} \\ & + \frac{1}{\varepsilon^2} \left\{ -\frac{2}{9} A_{g,3}^A - \frac{1}{3} \beta_1 G_{g,1}^A(\varepsilon) - \frac{4}{3} \beta_0 G_{g,2}^A(\varepsilon) \right\} + \frac{1}{\varepsilon} \left\{ \frac{1}{3} G_{g,3}^A(\varepsilon) \right\}, \end{aligned} \quad (28)$$

where $A_{g,i}^A$'s are the cusp anomalous dimensions and $G_{g,i}^A(\varepsilon)$ are the resummation functions which further decompose into $g_{g,j}^{A,i}$'s, and collinear (B_g^A), soft (f_g^A) and UV (γ_g^A) anomalous dimensions [24, 71, 83]. Here, f_g^A 's were introduced for the first time in the article [76]. The article [76] has shown that f_g^A 's fulfill the maximally non-Abelian property up to two loop level whose validity is reconfirmed in [83] at three loop level. All these f_g can be found in [76, 83], $A_{g,i}$ in [83–86] and $B_{g,i}$ in [83, 85] up to three loop level.

For NSV cross-section, we need the $g_{g,j}^{A,i}$'s which appear in the $G_{g,i}^A(\varepsilon)$ resummation functions. For N³LO calculations, $g_{g,3}^{A,1}$ is needed in addition to the quantities arising from one and two loops. The form factors for the pseudoscalar production up to two loop can be found in [76] and the three loop one is calculated in the article [38] by some of us. However, in this computation of SV+NSV cross-section at N³LO, the form factor is needed in a definite form which is slightly different from the one presented in this recent article [38]. With little bit of effort, the required form can be extracted from the above mentioned recent work. The $g_{g,i}^{A,k}$'s up to three loop level are given below [24] :

$$\begin{aligned} g_{g,1}^{A,1} &= C_A \left\{ 4 + \zeta_2 \right\}, \\ g_{g,1}^{A,2} &= C_A \left\{ -6 - \frac{7}{3} \zeta_3 \right\}, \\ g_{g,1}^{A,3} &= C_A \left\{ 7 - \frac{1}{2} \zeta_2 + \frac{47}{80} \zeta_2^2 \right\}, \\ g_{g,2}^{A,1} &= C_A^2 \left\{ \frac{11882}{81} + \frac{67}{3} \zeta_2 - \frac{44}{3} \zeta_3 \right\} + C_A n_f \left\{ -\frac{2534}{81} - \frac{10}{3} \zeta_2 - \frac{40}{3} \zeta_3 \right\} \\ &\quad + C_F n_f \left\{ -\frac{160}{3} + 12 \ln \left(\frac{\mu_R^2}{m_t^2} \right) + 16 \zeta_3 \right\}, \\ g_{g,2}^{A,2} &= C_F n_f \left\{ \frac{2827}{18} - 18 \ln \left(\frac{\mu_R^2}{m_t^2} \right) - \frac{19}{3} \zeta_2 - \frac{16}{3} \zeta_2^2 - \frac{128}{3} \zeta_3 \right\} + C_A n_f \left\{ \frac{21839}{243} - \frac{17}{9} \zeta_2 \right. \\ &\quad \left. + \frac{259}{60} \zeta_2^2 + \frac{766}{27} \zeta_3 \right\} + C_A^2 \left\{ -\frac{223861}{486} + \frac{80}{9} \zeta_2 + \frac{671}{120} \zeta_2^2 + \frac{2111}{27} \zeta_3 + \frac{5}{3} \zeta_2 \zeta_3 - 39 \zeta_5 \right\}, \\ g_{g,3}^{A,1} &= n_f C_J^{(2)} \left\{ -6 \right\} + C_F n_f^2 \left\{ \frac{12395}{27} - \frac{136}{9} \zeta_2 - \frac{368}{45} \zeta_2^2 - \frac{1520}{9} \zeta_3 - 24 \ln \left(\frac{\mu_R^2}{m_t^2} \right) \right\} \\ &\quad + C_F^2 n_f \left\{ \frac{457}{2} + 312 \zeta_3 - 480 \zeta_5 \right\} + C_A^2 n_f \left\{ -\frac{12480497}{4374} - \frac{2075}{243} \zeta_2 - \frac{128}{45} \zeta_2^2 \right. \\ &\quad \left. - \frac{12992}{81} \zeta_3 - \frac{88}{9} \zeta_2 \zeta_3 + \frac{272}{3} \zeta_5 \right\} + C_A^3 \left\{ \frac{62867783}{8748} + \frac{146677}{486} \zeta_2 - \frac{5744}{45} \zeta_2^2 - \frac{12352}{315} \zeta_3 \right\} \end{aligned}$$

$$\begin{aligned}
& -\frac{67766}{27}\zeta_3 - \frac{1496}{9}\zeta_2\zeta_3 - \frac{104}{3}\zeta_3^2 + \frac{3080}{3}\zeta_5 \Big\} + C_A \mathbf{n}_f^2 \Big\{ \frac{514997}{2187} - \frac{8}{27}\zeta_2 + \frac{232}{45}\zeta_2^2 \\
& + \frac{7640}{81}\zeta_3 \Big\} + C_A C_F \mathbf{n}_f \Big\{ -\frac{1004195}{324} + \frac{1031}{18}\zeta_2 + \frac{1568}{45}\zeta_2^2 + \frac{25784}{27}\zeta_3 + 40\zeta_2\zeta_3 + \frac{608}{3}\zeta_5 \\
& + 132 \ln \left(\frac{\mu_R^2}{m_t^2} \right) \Big\}.
\end{aligned} \tag{29}$$

C. Mass Factorization Kernel

The partonic cross-section $\Delta_{gg}^{A,NSV}(z, q^2, \mu_R^2, \mu_F^2)$ is UV finite after performing the coupling constant and overall operator renormalization using Z_{a_s} and Z_g^A . But it still exhibits collinear divergences and thus, requires mass factorization to remove them. In this section, the issue of collinear divergences is dealt with and we describe a prescription to remove them. The collinear singularities that arise in the massless limit of partons are removed in the \overline{MS} scheme using the mass factorization kernel $\Gamma(\hat{a}_s, \mu^2, \mu_F^2, z, \varepsilon)$. The kernel satisfies the following RG equation [24, 29] :

$$\mu_F^2 \frac{d}{d\mu_F^2} \Gamma(z, \mu_F^2, \varepsilon) = \frac{1}{2} P(z, \mu_F^2) \otimes \Gamma(z, \mu_F^2, \varepsilon), \tag{30}$$

where $P(z, \mu_F^2)$ are the Altarelli-Parisi (AP) splitting functions (matrix valued). We can expand $P(z, \mu_F^2)$ and $\Gamma(z, \mu_F^2, \varepsilon)$ in powers of the strong coupling constant a_s as follows :

$$P(z, \mu_F^2) = \sum_{i=1}^{\infty} a_s^i(\mu_F^2) P^{(i-1)}(z), \tag{31}$$

and

$$\Gamma(z, \mu_F^2, \varepsilon) = \delta(1-z) + \sum_{i=1}^{\infty} \hat{a}_s^i \left(\frac{\mu_F^2}{\mu^2} \right) S_\varepsilon^i \Gamma^{(i)}(z, \varepsilon). \tag{32}$$

We can solve the RGE for this mass factorization kernels. The solutions in the \overline{MS} scheme contains only the poles in ε and are given in [29]. The relevant values of the observable that are required for this computation are available in the articles [84, 85]. Only the diagonal AP kernels contribute to our analysis. So, we expand the corresponding AP splitting functions around $z = 1$ and all those terms that do not contribute to NSV are dropped.

The AP splitting functions near $z = 1$ for the gluon fusion sub-process take the following form [69]:

$$\begin{aligned}
P_{gg,i}(z, a_s(\mu_F^2)) = & 2 \left[B_{g,i}(a_s(\mu_F^2)) \delta(1-z) + A_{g,i} \mathcal{D}_0(z) \right. \\
& \left. + C_{g,i}(a_s(\mu_F^2)) \log(1-z) + D_{g,i}(a_s(\mu_F^2)) \right] + \mathcal{O}(1-z),
\end{aligned} \tag{33}$$

where $C_{g,i}$ and $D_{g,i}$ are constants that can be obtained from the splitting functions $P_{gg,i}$. Just as the cusp and the collinear anomalous dimensions were expanded in powers of $a_s(\mu_F^2)$, the constants C_g and D_g can also be expanded similarly as below:

$$C_g(a_s(\mu_F^2)) = \sum_{i=1}^{\infty} a_s^i(\mu_F^2) C_{g,i}, \quad D_g(a_s(\mu_F^2)) = \sum_{i=1}^{\infty} a_s^i(\mu_F^2) D_{g,i}, \tag{34}$$

where $C_{g,i}$ and $D_{g,i}$ to third order are available in [84, 85].

D. Soft Collinear Distribution

The resulting expression obtained after using the operator renormalization constant and mass factorization kernel is still not completely finite. It contains some residual divergences which get canceled against the contribution arising

from soft gluon emissions. This is why the finiteness of $\Delta_{gg}^{A,NSV}(z, q^2, \mu_R^2, \mu_F^2)$ in the limit $\varepsilon \rightarrow 0$ requires the soft-collinear distribution $\Phi_g(\hat{a}_s, q^2, \mu^2, z, \varepsilon)$ which has pole structure in ε similar to that of residual divergences. The distribution $\Phi_g(\hat{a}_s, q^2, \mu^2, z, \varepsilon)$ satisfies the K+G type differential equation [69]:

$$q^2 \frac{d}{dq^2} \Phi_g = \frac{1}{2} \left[\overline{K}_g \left(\hat{a}_s, \frac{\mu_R^2}{\mu^2}, \varepsilon, z \right) + \overline{G}_g \left(\hat{a}_s, \frac{q^2}{\mu_R^2}, \frac{\mu_R^2}{\mu^2}, \varepsilon, z \right) \right], \quad (35)$$

where \overline{K}_g contains all the divergent terms and \overline{G}_g contains all finite functions of (z, ε) . A detailed study has been given in [69].

We can rewrite $\Phi_g(\hat{a}_s, q^2, \mu^2, z, \varepsilon)$ in a convenient form which separates SV terms from the NSV. Hence, we decompose it as

$$\Phi_g = \Phi_g^{SV} + \Phi_g^{NSV}, \quad (36)$$

such that Φ_g^{SV} contains only SV terms and the remaining Φ_g^{NSV} contains next to soft-virtual terms in the limit $z \rightarrow 1$. The form of Φ_g^{SV} is given by

$$\Phi_g^{SV}(\hat{a}_s, q^2, \mu^2, z, \varepsilon) = \sum_{i=1}^{\infty} \hat{a}_s^i \left(\frac{q^2(1-z)^2}{\mu^2} \right)^{i\frac{\varepsilon}{2}} S_\varepsilon^i \left(\frac{i\varepsilon}{1-z} \right) \hat{\phi}_g^{SV,(i)}(\varepsilon), \quad (37)$$

where the expressions for $\hat{\phi}_g^{SV,(i)}(\varepsilon)$'s are explicitly given in Appendix B.

As verified by some of us (upto N³LO) [24], due to the universality of the soft gluon contribution, $\Phi_g^{SV}(\hat{a}_s, q^2, \mu^2, z, \varepsilon)$ must be the same as that of the Higgs boson production in gluon fusion:

$$\begin{aligned} \Phi_g^A &= \Phi_g^H = \Phi_g, \\ \text{i.e. } \overline{\mathcal{G}}_{g,i}^{A,k} &= \overline{\mathcal{G}}_{g,i}^{H,k} = \overline{\mathcal{G}}_{g,i}^k. \end{aligned} \quad (38)$$

Here, Φ_g^H and $\overline{\mathcal{G}}_{g,i}^{H,k}$ can be used for any gluon fusion process as these are independent of the operator insertion. The constants $\overline{\mathcal{G}}_{g,1}^{H,1}, \overline{\mathcal{G}}_{g,1}^{H,2}, \overline{\mathcal{G}}_{g,2}^{H,1}$ are determined from the result of the explicit computations of soft gluon emission to the Higgs boson production [87] and later these corrections were extended to all orders in dimensional regularization parameter ε in the article [40], using which $\overline{\mathcal{G}}_{g,1}^{H,3}$ and $\overline{\mathcal{G}}_{g,2}^{H,2}$ are extracted in [24]. The third order constant $\overline{\mathcal{G}}_{g,3}^{H,1}$ is computed from the result of SV cross-section for the production of the Higgs boson at N³LO [88] which was presented in the article [41]. The $\overline{\mathcal{G}}_{g,i}^{A,k}$ required to get the SV cross-sections up to N³LO are given in [24].

Now we move on to calculate the NSV part of the cross-section. The form of Φ_g^{NSV} is given by [69],

$$\Phi_g^{NSV}(\hat{a}_s, q^2, \mu^2, z, \varepsilon) = \sum_{i=1}^{\infty} \hat{a}_s^i \left(\frac{q^2(1-z)^2}{\mu^2} \right)^{i\frac{\varepsilon}{2}} S_\varepsilon^i \varphi_g^{NSV,(i)}(z, \varepsilon). \quad (39)$$

The coefficients $\varphi_g^{NSV,(i)}(z, \varepsilon)$ can be expressed as a sum of singular and finite part in ε given by,

$$\varphi_g^{NSV,(i)}(z, \varepsilon) = \varphi_{s,g}^{NSV,(i)}(z, \varepsilon) + \varphi_{f,g}^{NSV,(i)}(z, \varepsilon), \quad (40)$$

where explicit expressions for the singular coefficients $\varphi_{s,g}^{NSV,(i)}(z, \varepsilon)$ are given in Appendix C.

The coefficients $\varphi_{f,g}^{NSV,(i)}(z, \varepsilon)$ are finite as $\varepsilon \rightarrow 0$ and can be written in terms of the finite coefficients $\mathcal{G}_{L,i}^g(z, \varepsilon)$ as [69],

$$\varphi_{f,g}^{NSV,(1)}(z, \varepsilon) = \frac{1}{\varepsilon} \mathcal{G}_{L,1}^g(z, \varepsilon), \quad (41)$$

$$\varphi_{f,g}^{NSV,(2)}(z, \varepsilon) = \frac{1}{\varepsilon^2} \left\{ -\beta_0 \mathcal{G}_{L,1}^g(z, \varepsilon) \right\} + \frac{1}{2\varepsilon} \mathcal{G}_{L,2}^g(z, \varepsilon), \quad (42)$$

$$\begin{aligned} \varphi_{f,g}^{NSV,(3)}(z, \varepsilon) &= \frac{1}{\varepsilon^3} \left\{ \frac{4}{3} \beta_0^2 \mathcal{G}_{L,1}^g(z, \varepsilon) \right\} + \frac{1}{\varepsilon^2} \left\{ -\frac{1}{3} \beta_1 \mathcal{G}_{L,1}^g(z, \varepsilon) - \frac{4}{3} \beta_0 \mathcal{G}_{L,2}^g(z, \varepsilon) \right\} \\ &\quad + \frac{1}{3\varepsilon} \mathcal{G}_{L,3}^g(z, \varepsilon), \end{aligned} \quad (43)$$

where

$$\mathcal{G}_{L,1}^g(z, \varepsilon) = \sum_{j=1}^{\infty} \varepsilon^j \mathcal{G}_{L,1}^{g,(j)}(z), \quad (44)$$

$$\mathcal{G}_{L,2}^g(z, \varepsilon) = -2\beta_0 \mathcal{G}_{L,1}^{g,(1)}(z) + \sum_{j=1}^{\infty} \varepsilon^j \mathcal{G}_{L,2}^{g,(j)}(z), \quad (45)$$

$$\mathcal{G}_{L,3}^g(z, \varepsilon) = -2\beta_1 \mathcal{G}_{L,1}^{g,(1)}(z) - 2\beta_0 \left(\mathcal{G}_{L,2}^{g,(1)}(z) + 2\beta_0 \mathcal{G}_{L,1}^{g,(2)}(z) \right) + \sum_{j=1}^{\infty} \varepsilon^j \mathcal{G}_{L,3}^{g,(j)}(z). \quad (46)$$

The coefficients $\mathcal{G}_{L,i}^{g,(j)}(z)$ in the above equations are parameterized in terms of $\log^k(1-z)$, $k = 0, 1, \dots$ and all other terms that vanish as $z \rightarrow 1$ are dropped

$$\mathcal{G}_{L,1}^{g,(j)}(z) = \sum_{k=0}^{i+j-1} \mathcal{G}_{L,i}^{g,(j,k)}(z) \log^k(1-z). \quad (47)$$

The highest power off the $\log(1-z)$ at every order depends on the order of the perturbation i.e. the power of a_s and also the power of ε at each order in a_s .

The expansion coefficients $\varphi_{g,i}^{(k)}$ are related to $\mathcal{G}_{L,i}^{g,(j,k)}$ as below [69]:

$$\varphi_{g,1}^{(k)} = \mathcal{G}_{L,1}^{g,(1,k)}, \quad k = 0, 1 \quad (48)$$

$$\varphi_{g,2}^{(k)} = \frac{1}{2} \mathcal{G}_{L,2}^{g,(1,k)} + \beta_0 \mathcal{G}_{L,1}^{g,(2,k)}, \quad k = 0, 1, 2 \quad (49)$$

$$\varphi_{g,3}^{(k)} = \frac{1}{3} \mathcal{G}_{L,3}^{g,(1,k)} + \frac{2}{3} \beta_1 \mathcal{G}_{L,1}^{g,(2,k)} + \frac{2}{3} \beta_0 \mathcal{G}_{L,2}^{g,(2,k)} + \frac{4}{3} \beta_0^2 \mathcal{G}_{L,1}^{g,(3,k)}, \quad k = 0, 1, 2, 3. \quad (50)$$

IV. NEXT TO SV RESULTS

Using all the above ingredients which are available, we can calculate the NSV coefficient functions for pseudoscalar higgs boson production from gluon fusion in terms of the $\varphi_{g,i}^{(k)}$'s defined above. The NSV correction to the production of pseudoscalar Higgs boson is available up to order a_s^2 and the SV correction is available up to order a_s^3 . On the contrary, the NSV corrections to the production of scalar Higgs boson are available up to order a_s^3 . As given in Eq. (13) of [25], we can obtain the pseudoscalar result from the available scalar higgs boson result using

$$\begin{aligned} \Delta_{gg}^{A,NSV}(z, q^2, \mu_R^2, \mu_F^2) &= \frac{g_0(a_s)}{g_0^H(a_s)} \left[\Delta_{gg}^{H,NSV}(z, q^2, \mu_R^2, \mu_F^2) \right. \\ &\quad \left. + \delta \Delta_{gg}^{A,NSV}(z, q^2, \mu_R^2, \mu_F^2) \right], \end{aligned} \quad (51)$$

where $\delta \Delta_{gg}^{A,NSV}(z, q^2, \mu_R^2, \mu_F^2) = 0$ for the threshold limit $z \rightarrow 1$, as can be seen in [25]. Eq. (51) effectively defines $\delta \Delta_{gg}^{A,NSV}(z, q^2, \mu_R^2, \mu_F^2)$ as the correction to the scalar Higgs coefficient functions such that the rescaling $g_0(a_s)/g_0^H(a_s)$ converts them to the pseudoscalar coefficients. Here, $\Delta_{gg}^{A,NSV}(z, q^2, \mu_R^2, \mu_F^2)$ represents that for pseudoscalar higgs boson and $\Delta_{gg}^{H,NSV}(z, q^2, \mu_R^2, \mu_F^2)$ represents the coefficient function for scalar higgs boson. Moreover, $g_0(a_s)$ is the constant function of resummation for pseudoscalar Higgs, and $g_0^H(a_s)$ is the analogous function for scalar

Higgs. The ratio $g_0(a_s)/g_0^H(a_s)$ is available up to a_s^3 order and is given below:

$$\begin{aligned}
\frac{g_0(a_s)}{g_0^H(a_s)} = & 1 + a_s(8C_A) + a_s^2 \left[\frac{1}{3} \left\{ 215C_A^2 - 20C_A^2 \log\left(\frac{q^2}{\mu_R^2}\right) - 2C_A n_f - 93C_F n_f \right. \right. \\
& \left. \left. - 4C_A n_f \log\left(\frac{q^2}{\mu_R^2}\right) - 12C_F n_f \log\left(\frac{q^2}{\mu_R^2}\right) + 36C_F n_f \log\left(\frac{\mu_R^2}{m_t^2}\right) \right\} \right] \\
& + a_s^3 \left[\frac{1}{81} \left\{ 68309C_A^3 - 18084C_A^3 \log\left(\frac{q^2}{\mu_R^2}\right) + 1980C_A^3 \left\{ \log\left(\frac{q^2}{\mu_R^2}\right) \right\}^2 \right. \right. \\
& + 1973C_A^2 n_f - 67094C_A C_F n_f + 6867C_F^2 n_f - 2514C_A^2 \log\left(\frac{q^2}{\mu_R^2}\right) n_f \\
& + 13428C_A C_F \log\left(\frac{q^2}{\mu_R^2}\right) n_f + 324C_F^2 \log\left(\frac{q^2}{\mu_R^2}\right) n_f + 36C_A^2 \left\{ \log\left(\frac{q^2}{\mu_R^2}\right) \right\}^2 n_f \\
& + 1188C_A C_F \left\{ \log\left(\frac{q^2}{\mu_R^2}\right) \right\}^2 n_f + 7776C_A C_F \log\left(\frac{\mu_R^2}{m_t^2}\right) n_f \\
& - 7128C_A C_F \log\left(\frac{q^2}{\mu_R^2}\right) \log\left(\frac{\mu_R^2}{m_t^2}\right) n_f - 631C_A n_f^2 + 4520C_F n_f^2 \\
& + 402C_A \log\left(\frac{q^2}{\mu_R^2}\right) n_f^2 - 2952C_F \log\left(\frac{q^2}{\mu_R^2}\right) n_f^2 - 72C_A \log\left(\frac{q^2}{\mu_R^2}\right)^2 n_f^2 \\
& - 216C_F \left\{ \log\left(\frac{q^2}{\mu_R^2}\right) \right\}^2 n_f^2 + 1296C_F \log\left(\frac{q^2}{\mu_R^2}\right) \log\left(\frac{\mu_R^2}{m_t^2}\right) n_f^2 - 324n_f C_J^{(2)} \\
& \left. \left. - 5616C_A^3 \zeta_3 - 1296C_A^2 n_f \zeta_3 + 6048C_A C_F n_f \zeta_3 + 864C_F^2 n_f \zeta_3 \right\} \right]. \tag{52}
\end{aligned}$$

So, we are able to evaluate the NSV coefficient function for pseudoscalar higgs boson production from gluons in two ways : (i) by using the formalism developed in [29, 69, 71] and (ii) by using the above ratio of $g_0(a_s)/g_0^H(a_s)$ and the combining it with the scalar Higgs NSV cross-section. After multiplying the Eq. (52) with the scalar higgs result, we can expand it order by order in a_s . We can then evaluate the $\varphi_{g,i}^{(k)}$ values by comparing the two results obtained by the above two distinct methods. The $\varphi_{g,i}^{(k)}$ values up to 2-loop and for the two highest logarithms in 3-loop are the same as the scalar higgs boson results for the corresponding $\varphi_{g,i}^{(k)}$ in Eq. (2.37) of [69] as expected. We get the following two new results of $\varphi_{g,i}^{(k)}$ for pseudoscalar higgs boson production from gluon fusion:

$$\begin{aligned}
\varphi_{g,3}^{(0)} = & C_A^2 n_f \left(-\frac{307187}{1458} + \frac{27320}{81} \zeta_2 - \frac{184}{15} \zeta_2^2 + 244\zeta_3 \right) - C_A n_f^2 \left\{ \frac{8}{729} \left(-196 \right. \right. \\
& \left. \left. + 1539\zeta_2 + 540\zeta_3 \right) \right\} + C_A^3 \left\{ \frac{563231}{729} + \frac{3488}{15} \zeta_2^2 - \frac{34292}{27} \zeta_3 + \frac{16}{81} \zeta_2 (-7100 \right. \\
& \left. + 297\zeta_3) + 192\zeta_5 \right\} + n_f \frac{1}{270} (-13265 + 1800\zeta_2 + 864\zeta_2^2 + 9240\zeta_3), \tag{53}
\end{aligned}$$

$$\begin{aligned}
\varphi_{g,3}^{(1)} = & \frac{2}{81} \left\{ 84C_A n_f^2 + 27n_f (-3 + 2\zeta_2) + C_A^2 n_f (845 - 1170\zeta_2 - 324\zeta_3) \right. \\
& \left. + C_A^3 (-9494 + 5760\zeta_2 + 6048\zeta_3) \right\}. \tag{54}
\end{aligned}$$

As depicted in Section 3 of [69], once we have the $\varphi_{g,i}^{(k)}$ values up to a certain order, we can predict the coefficients of the highest logarithms of the consecutive higher orders of $\Delta_{gg}^{A,NSV}(z, q^2, \mu_R^2, \mu_F^2)$ calculated using the formalisms developed in [29, 69, 71]. Using the above $\varphi_{g,i}^{(k)}$ values, we could predict the three highest logarithms of $\Delta_{gg}^{A,NSV}(z, q^2, \mu_R^2, \mu_F^2)$ up to order a_s^7 from order a_s^4 . These predictions match with the result obtained using the relation developed in [25]. The NSV coefficient functions calculated from the available Higgs boson results can be matched with that obtained using the developed formalism in [29, 69, 71]. Till order a_s^3 , the results match exactly using the above defined $\varphi_{g,i}^{(k)}$ values. To exactly match the other higher order results of the pseudoscalar higgs boson, the ingredients are still not available. So, we match the highest logarithms of the higher orders up to order a_s^7 .

from a_s^4 of the $\Delta_{gg}^{A,NSV}(z, q^2, \mu_R^2, \mu_F^2)$ result obtained from the two ways mentioned above. These do match and is a consistency check on the results obtained.

The explicit results of the NSV cross-section up to N³LO are given in the Appendix A where it can be seen that the general form of the output is depicted as :

$$\Delta_{g,i}^{A,NSV}(z, q^2) = \delta(1-z)[\dots] + \sum_{j=1/2,1,\dots}^i \mathcal{D}_{(2j-1)}[\dots] + \sum_{j=1/2,1,\dots}^i \log^{(2j-1)}(1-z)[\dots]. \quad (55)$$

where $i = 1, 2, 3$. and $[\dots]$ represents coefficients of the corresponding distribution, logarithmic term or delta function. The constant terms in the above result actually correspond to $\log^0(1-z)$ coefficients.

V. RESUMMATION OF THE NSV RESULTS IN MELLIN SPACE

In order to study the all order behavior of Δ_g in N-moment space, it is convenient to use the following form of the partonic coefficient function [69]:

$$\Delta_g(q^2, \mu_R^2, \mu_F^2, z) = C_0^g(q^2, \mu_R^2, \mu_F^2) \mathcal{C} \exp \left(2\Psi_D^g(q^2, \mu_F^2, z) \right), \quad (56)$$

where

$$\Psi_D^g(q^2, \mu_F^2, z) = \frac{1}{2} \int_{\mu_F^2}^{q^2(1-z)^2} \frac{d\lambda^2}{\lambda^2} P_{gg}(a_s(\lambda^2), z) + \mathcal{Q}^g(a_s(q^2(1-z)^2), z), \quad (57)$$

with

$$\mathcal{Q}^g(a_s(q^2(1-z)^2), z) = \left(\frac{1}{1-z} \overline{G}_{SV}^g(a_s(q^2(1-z)^2)) \right)_+ + \varphi_{f,g}(a_s(q^2(1-z)^2), z). \quad (58)$$

The coefficient C_0^g is z independent coefficient and is expanded in powers of $a_s(\mu_R^2)$ as

$$C_0^g(q^2, \mu_R^2, \mu_F^2) = \sum_{i=0}^{\infty} a_s^i(\mu_R^2) C_{0i}^g(q^2, \mu_R^2, \mu_F^2), \quad (59)$$

where the coefficients C_{0i}^g are calculated in [38] for pseudoscalar. Eq.(56) gives the z -space resummed result.

Now it is easy to compute the Mellin moment of Δ_g . The limit $z \rightarrow 1$ translates to $N \rightarrow \infty$ in the N -moment space and to include NSV terms, we need to keep $\mathcal{O}(1/N)$ corrections in the large N limit. The Mellin moment of Δ_g is given by [69]

$$\Delta_{g,N}(q^2, \mu_R^2, \mu_F^2) = C_0(q^2, \mu_R^2, \mu_F^2) \exp(\Psi_N^g(q^2, \mu_F^2)), \quad (60)$$

The Mellin moment of the exponent acquires the following form:

$$\Psi_N^g = \Psi_{SV,N}^g + \Psi_{NSV,N}^g, \quad (61)$$

where we can split Ψ_N^g in such a way that all those terms that are functions of $\log^j(N)$, $j = 0, 1, \dots$ are kept in $\Psi_{SV,N}^g$ and the remaining terms that are proportional to $(1/N) \log^j(N)$, $j = 0, 1, \dots$ are contained in $\Psi_{NSV,N}^g$. Hence,

$$\Psi_{SV,N}^g = \log(g_0^g(a_s(\mu_R^2))) + g_1^g(\omega) \log(N) + \sum_{i=0}^{\infty} a_s^i(\mu_R^2) g_{i+2}^g(\omega), \quad (62)$$

where $g_i^g(\omega)$ are identical to those in [47, 54, 89] obtained from the resummed formula for SV terms and $g_0^g(a_s)$ is expanded in powers of a_s as (see [49])

$$\log(g_0^g(a_s(\mu_R^2))) = \sum_{i=1}^{\infty} a_s^i(\mu_R^2) g_{0,i}^g. \quad (63)$$

The $g_0^g(a_s(\mu_R^2))$ are also provided in the ancillary files of [69]. Here the function $\Psi_{\text{NSV},N}^g$ is given by

$$\Psi_{\text{NSV},N}^g = \frac{1}{N} \sum_{i=0}^{\infty} a_s^i(\mu_R^2) \left(\bar{g}_{i+1}^g(\omega) + h_i^g(\omega, N) \right), \quad (64)$$

with

$$h_i^g(\omega, N) = \sum_{k=0}^i h_{ik}^g(\omega) \log^k(N). \quad (65)$$

where the resummation constants, $\bar{g}_i^g(\omega)$ and $h_i^g(\omega, N)$, are given in [69].

VI. NUMERICAL RESULTS AND DISCUSSION

In this section, we will present our numerical results of the NSV corrections at N³LO level in QCD for the production of a pseudoscalar Higgs boson at the LHC. Our predictions are based on EFT where the top quarks are integrated out at higher orders. However, we retain the top quark mass dependence at LO. The term $C_f^{(2)}$ in the Wilson coefficient is taken to be zero in our analysis because it is not available in the literature yet. For simplicity, we have set $\cot \beta = 1$ in our numerical analysis. Results for other values of $\cot \beta$ can be easily obtained by rescaling the cross-sections with $\cot^2 \beta$. At LO we have retained the full top quark mass dependence while EFT approach has been used for higher order corrections. We use MMHT 2014 PDFs throughout where the LO, NLO and NNLO parton level cross-sections are convoluted with the corresponding order by order central PDF sets, while for N³LO cross-sections we simply use MMHT2014nnlo68cl PDFs. The strong coupling constant is provided by the respective PDFs from LHAPDF.

To estimate the impact of QCD corrections, we define the K-factors as

$$K_{(1)}^X = \frac{\sigma_{\text{NLO}}^X}{\sigma_{\text{LO}}}, \quad K_{(2)}^X = \frac{\sigma_{\text{NNLO}}^X}{\sigma_{\text{LO}}}, \quad (66)$$

where X is either SV or SV+NSV or Full which includes all possible sub-processes or Full(gg) which includes only the gluon-gluon(gg) sub-process. When the Full(gg) case is considered, only the gg sub-process is taken at the n -th order while at all other sub-processes are considered at the lower orders ($k < n$).

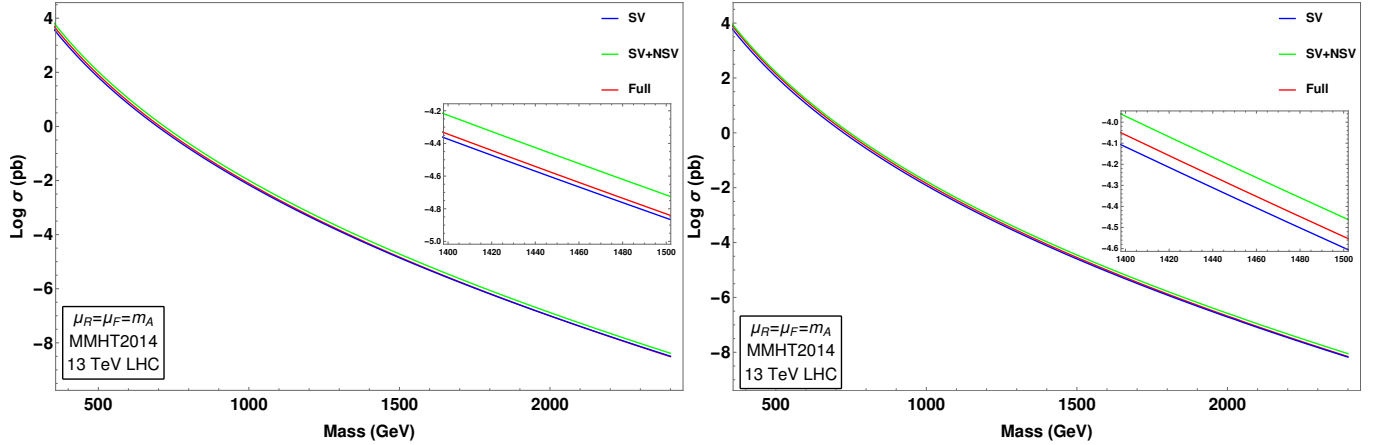


FIG. 1: Pseudoscalar production cross-section at (a) NLO level (left panel) and (b) NNLO level (right panel) with a comparison between fixed order SV, SV+NSV and Full results at 13 TeV LHC

In Fig. 1, we plot the pseudoscalar production cross-section as a function of its mass m_A at NLO(left panel) and at NNLO (right panel), by varying m_A from 350 GeV to 2400 GeV. Here the “SV” results do contain the SV threshold logarithms and $\delta(1-z)$ contributions, while the “NSV” corrections include the NSV logarithms in the gluon fusion channel only. We note that the NSV corrections at higher orders do also arise from other partonic channels, a detailed study of which is beyond the scope of the present work and will be presented elsewhere. As seen from figures, the

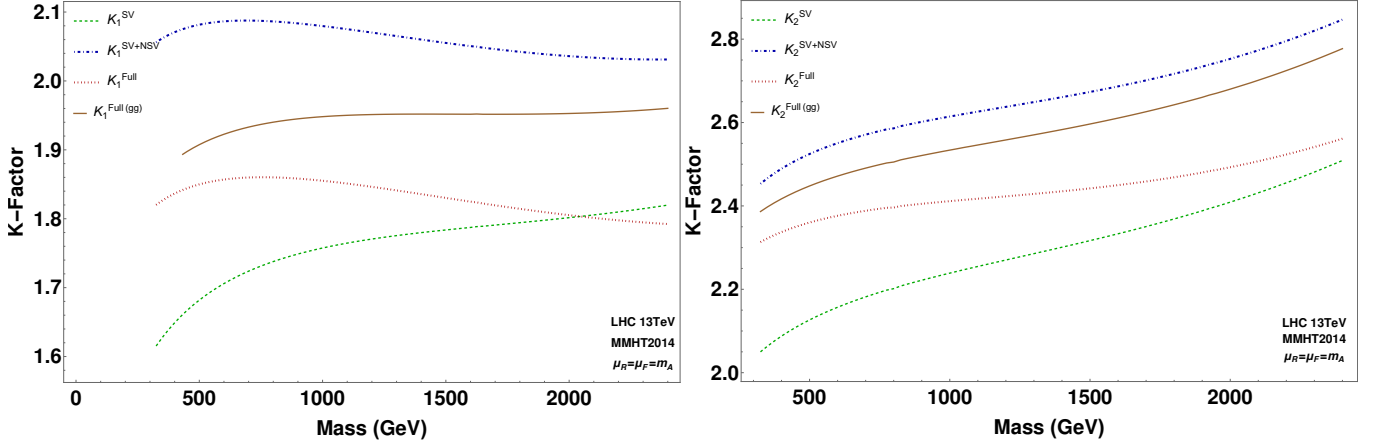


FIG. 2: K-Factor for Pseudoscalar production cross-section at (a) NLO level (left panel) and (b) NNLO level (right panel) with a comparison between fixed order SV, SV+NSV, Full (all sub-processes included) and Full (only gg sub-process included) results at 13 TeV LHC.

SV results give sizable contribution to the fixed order results however they underestimate the latter. The inclusion of NSV corrections increases the cross-section substantially but they overestimate the FO results for the mass range of m_A we have considered.

To study better the impact of these corrections at SV and beyond, we depict in Fig. 2 the corresponding K-factors defined in Eq. 66. Since our NSV corrections include only gluon fusion channel, it is worthwhile to have comparison with the complete result of the gluon fusion channel including the pure regular contributions. From these K-factors, we notice that the SV corrections converge to the FO result (denoted by K_i^{Full}) in the high mass region and differ significantly in the small mass region. However, the FO result here also does contain contribution from other parton channels, and the difference noticed between the full FO result and the pure gluon channel (denoted by $K_i^{Full(gg)}$) contribution can be understood from the presence of these other channels. We also notice that the SV+NSV corrections have similar behavior to that of complete gluon fusion channel contribution, with the former being a little bit higher than the latter. This also indicates that the regular or beyond NSV corrections are sizable at higher orders as well as they are negative for the process under consideration.

Next, we study the impact of resummation of these NSV logarithms on the pseudoscalar production cross-section at NLL and NNLL accuracy. For the resummed cross-section, we do the matching as below :

$$\sigma^{(\text{matched})} = \sigma_{\text{resum}}^{\text{SV+NSV}} - \sigma^{\text{SV+NSV}} \Big|_{(\text{FO})} + \sigma^{(\text{FO})}. \quad (67)$$

In Fig. 3, we depict the resummed K-factors at NLO and NNLO orders and contrast them against the corresponding ones due to the SV resummation for a wide range of pseudoscalar mass i.e. $200 < m_A < 3000$ GeV. We define these K-factors as

$$K_{(1)}^{\text{resum}} = \frac{\sigma_{\text{NLO+NLL}}}{\sigma_{\text{LO}}}, \quad K_{(2)}^{\text{resum}} = \frac{\sigma_{\text{NNLO+NNLL}}}{\sigma_{\text{LO}}},$$

$$\bar{K}_{(1)}^{\text{resum}} = \frac{\sigma_{\text{NLO+NLL}}}{\sigma_{\text{LO}}}, \quad \bar{K}_{(2)}^{\text{resum}} = \frac{\sigma_{\text{NNLO+NNLL}}}{\sigma_{\text{LO}}}, \quad (68)$$

The resummed NLO SV K-factor ($K_{(1)}^{\text{resum}}$) varies from 2.2 (at $m_A = 200$ GeV) to about 2.6 (at $m_A = 3000$ GeV). However, the inclusion of NSV logarithms at $\overline{\text{NLL}}$ accuracy increase these results by about 30% in the low mass region and by about 40% of LO in the high mass region i.e. ($\bar{K}_{(1)}^{\text{resum}}$) varies from 2.5 to about 2.9. The resummation of NSV logarithms to $\overline{\text{NNLL}}$ accuracy has similar behavior and enhance the SV resummed results by about 20% (40%) in the low (high) mass region.

We will next study theoretical uncertainties due to unphysical scales μ_R and μ_F in our predictions. We will present the conventional seven point scale uncertainties and make the following scale choices ($\mu_R/m_A, \mu_F/m_A$) : (0.5, 0.5), (0.5, 1), (1.0, 0.5), (1.0, 1.0), (1.0, 2.0), (2.0, 1.0) and (2.0, 2.0) for a given value of m_A . We note that for NSV

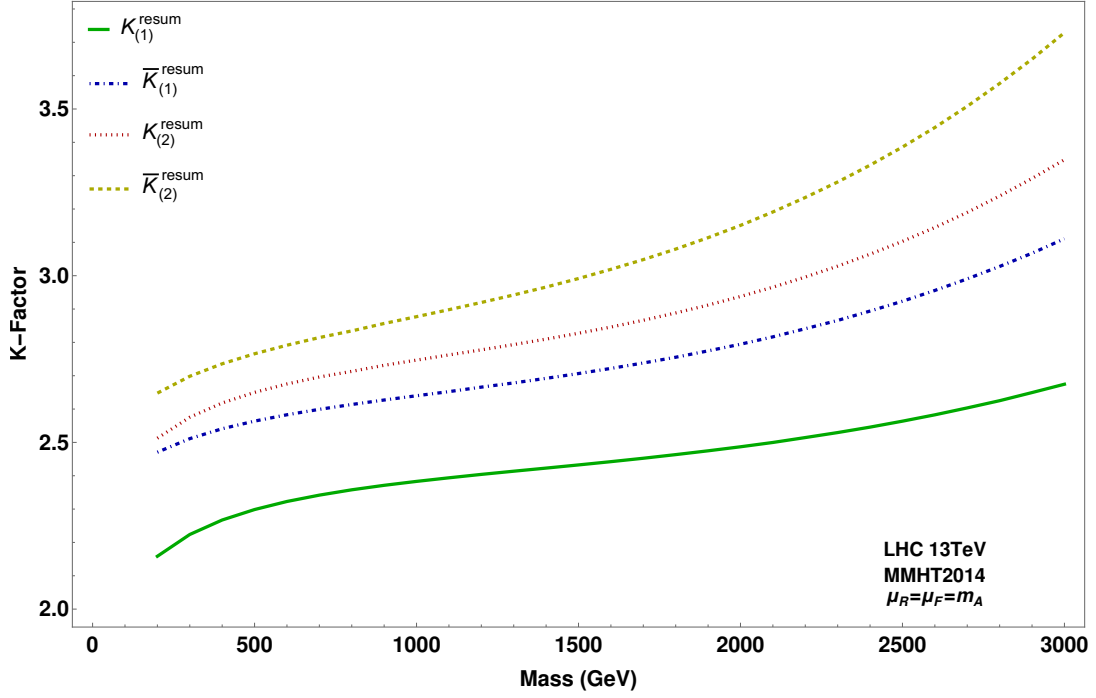


FIG. 3: Resummed K-factor plot at NLO (K_1) and NNLO (K_2) levels at 13 TeV LHC taking MMHT 2014 as the reference PDF and choosing the central scale $\mu_R = \mu_F = m_A$.

LO	54.92	34.70
NLO	34.61	25.81
NNLO	18.18	14.96
LO+LL	61.84	43.35
NLO+NLL	28.45	18.80
NNLO+NNLL	13.89	6.42
LO+LL	64.39	45.83
NLO+NLL	38.52	18.13
NNLO+NNLL	31.62	1.81

TABLE I: Percentage Uncertainty in data at mass $m_A=700$ GeV for the 7-point scale uncertainty (2nd column) and the μ_F scale fixed case (3rd column) at 13 TeV LHC with MMHT 2014 PDF.

resummation done in this analysis, logarithms involving factorization scale gets resummed to all orders only for the gluon channel. However, the factorization scale dependence also enters through other parton channels which are not included in our present analysis. In this context, we also study the scale uncertainties by varying μ_R and keeping μ_F at a fixed scale. So, in the latter case, the scale choices we make are $\mu_R = (0.5, 1.0, 2.0) m_A$ for $\mu_F = 125$ GeV, 700 GeV.

In Fig. 4 we present the 7-point scale uncertainties in the top panel and those due to the μ_R in the bottom panel for the pseudoscalar mass $m_A = 125$ GeV. All these uncertainties are presented to NNLO+NNLL and NNLO+NNLL accuracy. In all the uncertainty plots, the first three results correspond to the FO results, the next three correspond to the SV resummation and the last three results represent the NSV resummed ones. We plot the uncertainty involved for the total pseudoscalar production cross-section at each order. In Fig. 5, we show similar results as those in Fig. 4 with the only difference being the mass of the pseudoscalar which is now taken to be $m_A = 700$ GeV.

In the table I, we tabulate the percentage errors due to the 7-point scale uncertainty and μ_F scale fixed case for mass $m_A = 700$ GeV. From this table we can see that the percentage errors reduce considerably from the 7-point scale uncertainty case to the μ_F scale fixed case. This reduction can be attributed to the fact that several other partonic channels are involved in 7-point scale uncertainty which are not considered in this analysis.

For completeness we also estimate the uncertainty due to the choice of parton densities in our calculation. Fig. 6 depicts the PDF uncertainties involved in the calculations due to the choice of different PDF sets. For this analysis,

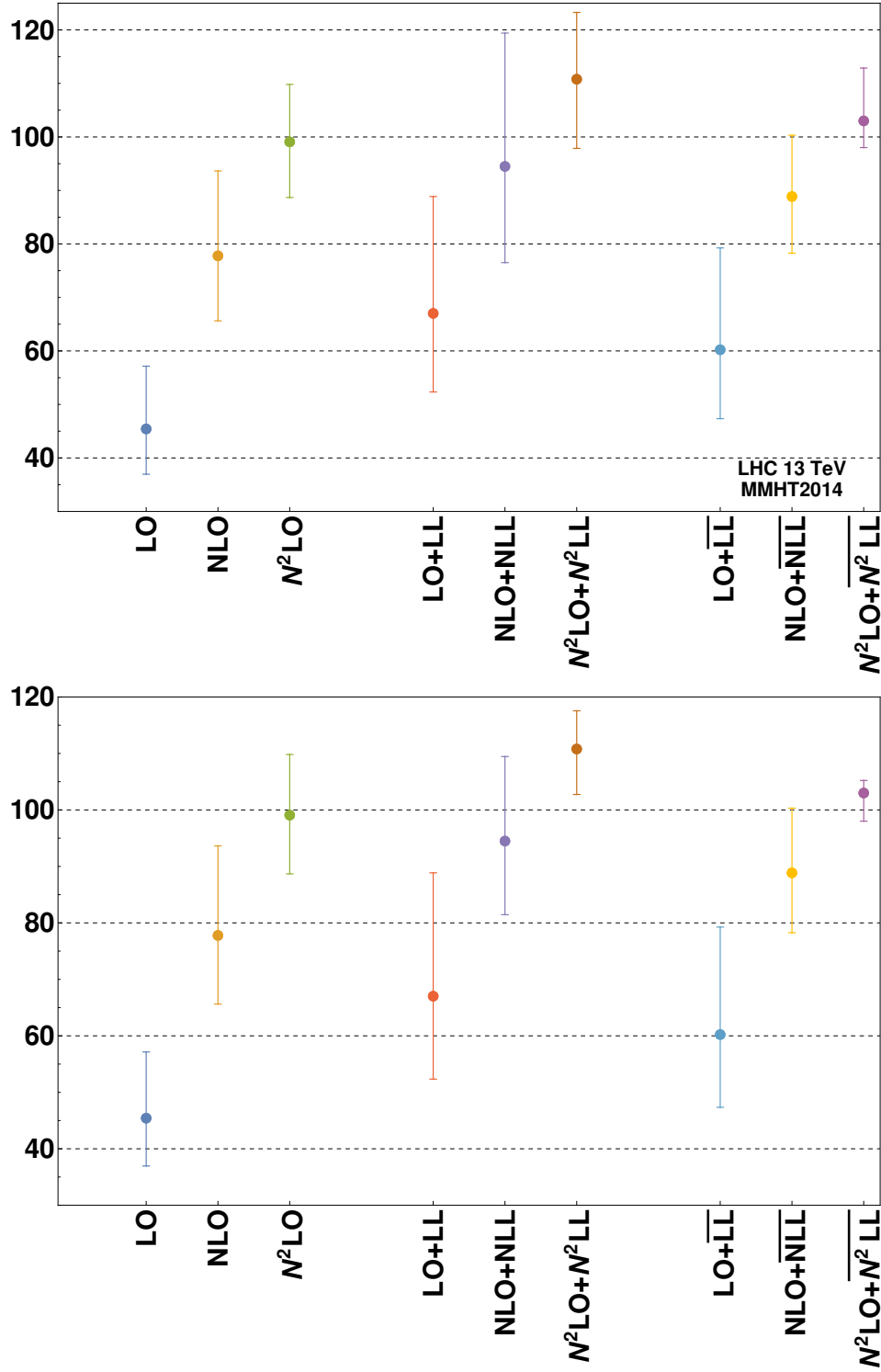


FIG. 4: Uncertainty plot with two different scale choices for $m_A=125$ GeV at 13 TeV LHC with MMHT 2014 PDF : (a) 7-point scale uncertainty (top figure) and (b) μ_F scale fixed (bottom figure).

we choose NNPDF30, PDF4LHC15, HERAPDF20, CT14, ABMP16 as the reference PDF's and present the results for the production cross-section at NNLO+NLL normalized with the corresponding results obtained from our default choice of *MMHT* 2014 PDF set.

Finally, we attempt to give predictions for the pseudoscalar production cross-section after including the resummed

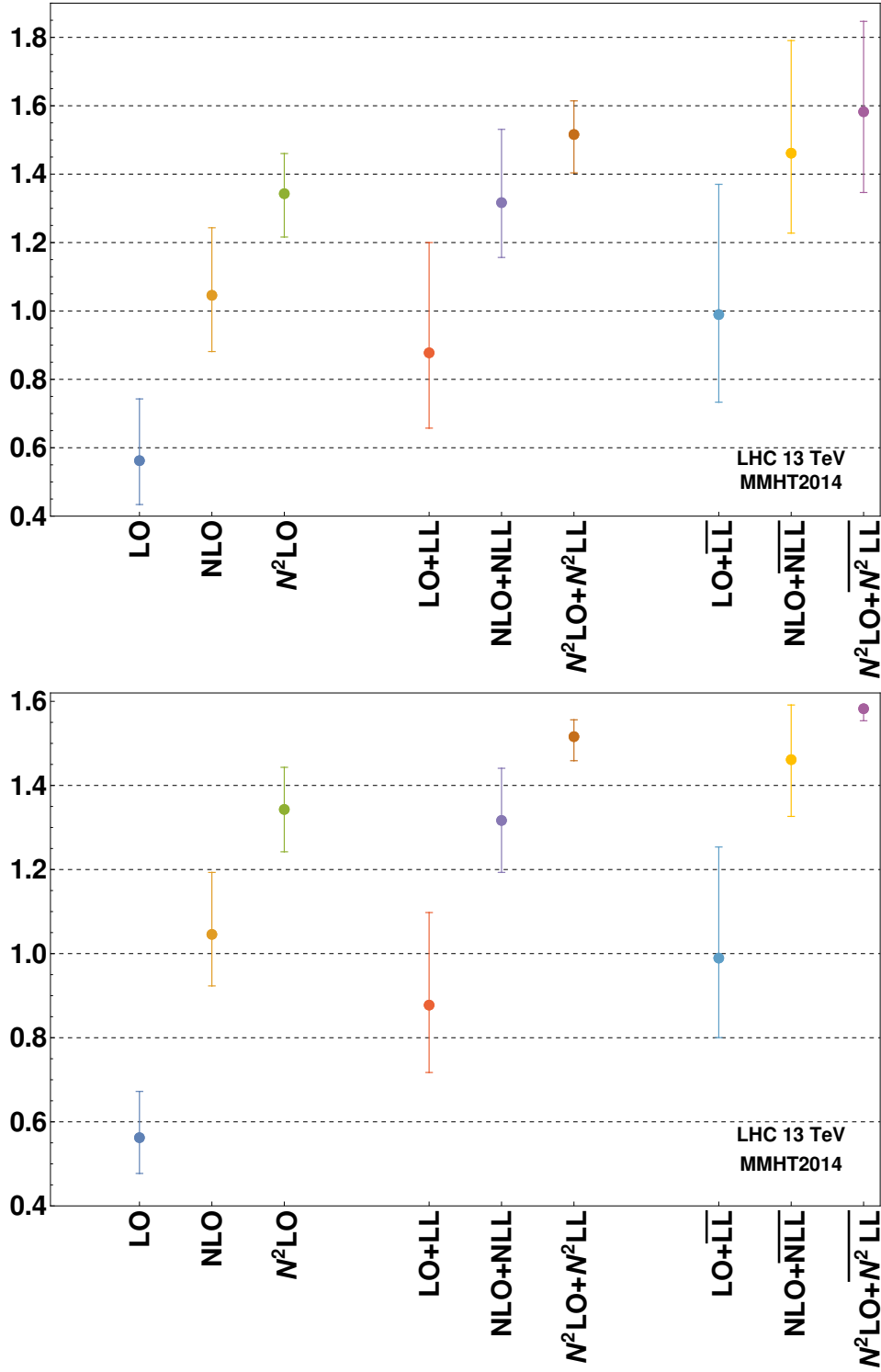


FIG. 5: Uncertainty plot with two different scale choices for $m_A=700$ GeV at 13 TeV LHC with MMHT 2014 PDF : (a) 7-point scale uncertainty (top figure) and (b) μ_F scale fixed (bottom figure).

results to $\overline{N^3LL}$ level and then matching them to the FO N^3LO_A results. Here, N^3LO_A results represent the approximate full FO result at third order in QCD which we have taken from the public code [90–94]. In the left panel of Fig. 7, we plot the pseudoscalar production cross-section as a function of its mass m_A at third order and present the results upto $N^3LO_A + \overline{N^3LL}$. In the right panel we give the corresponding K-factors obtained from LO cross-sections.

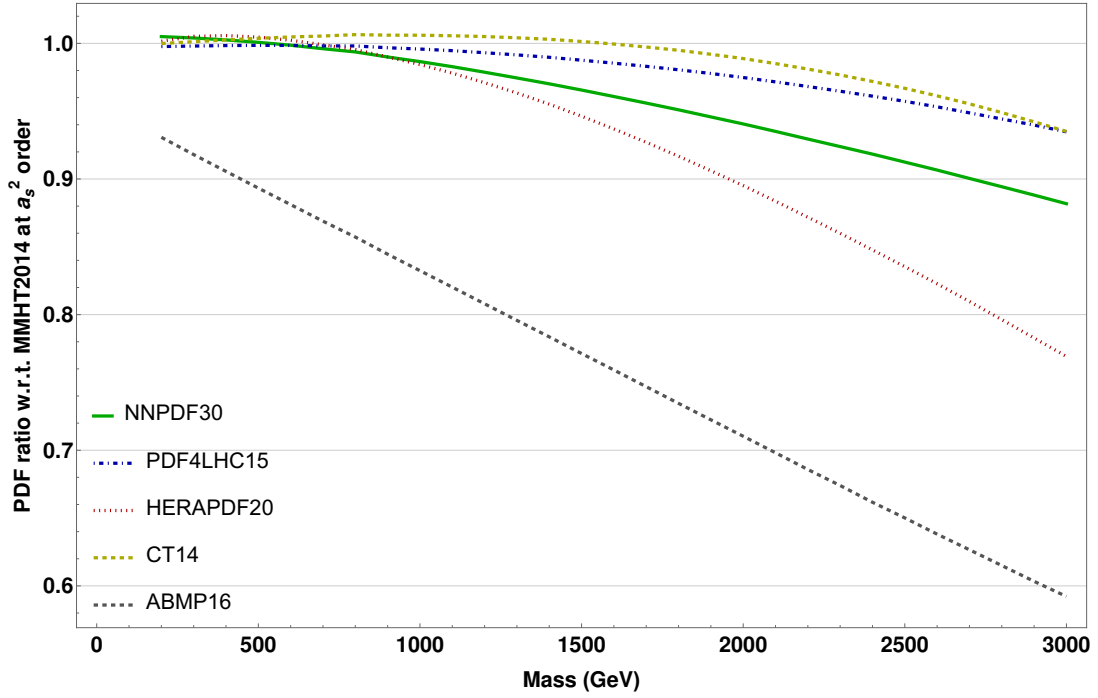


FIG. 6: Percentage uncertainty in the Pseudoscalar production cross-section at NNLO level with different PDFs taking MMHT 2014 as the mean.

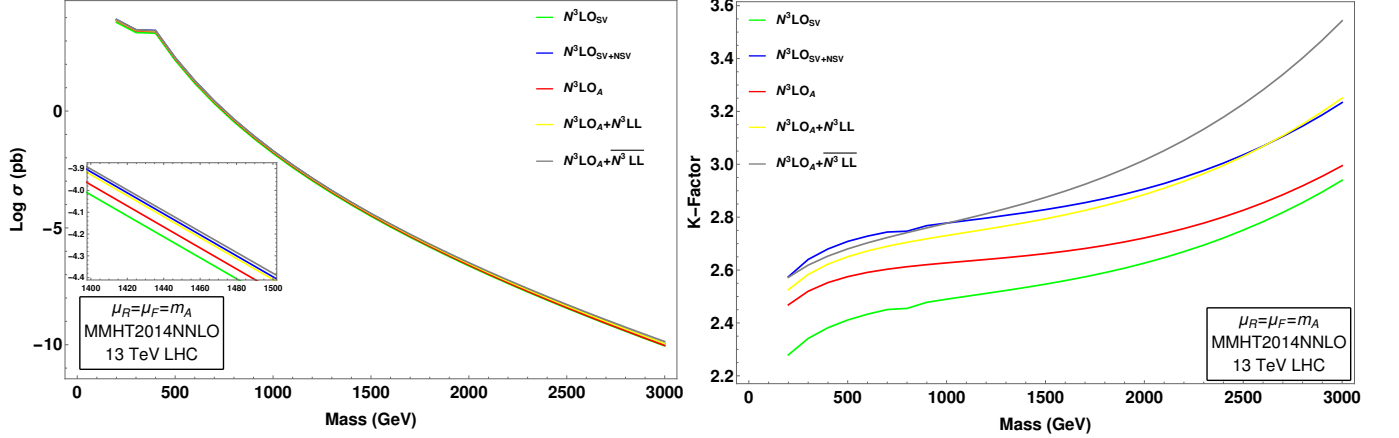


FIG. 7: (a) Pseudoscalar production cross-section at third order in QCD (left panel) and (b) the corresponding K-Factors (right panel). The corresponding resummed results to N^3LL accuracy are also given after matching them to the approximate full N^3LO_A results.

We also give K-factors for FO case by keeping only the third-order SV and SV+NSV results and comparing them with those of N^3LO_A . The N^3LO_{SV} results are closer to the N^3LO_A ones in the high mass region, while N^3LO_{SV+NSV} results are closer to the N^3LO_A ones in the small mass region. We observe that the inclusion of NSV corrections either at the FO level or their resummation through NSV substantially increases the cross-sections. However, a detailed phenomenological study at N^3LL level accuracy including the estimation of theoretical uncertainties requires additional terms such as the resummation constant $h_{33}^g(\omega)$ that are yet to be determined.

In each of the above cases, the N^3LO level PDF's are not available yet. However, it can be anticipated that the uncertainty will get further reduced if the full N^3LO results with the corresponding PDF's are made available.

VII. SUMMARY

In this work, we have performed the NSV resummation for pseudoscalar production process to $\overline{\text{NNLL}}$ accuracy in QCD at the LHC. We further make a detailed phenomenology of the same and present our results for 13 TeV LHC. We have computed the NSV corrections at both first and second orders in QCD and compared them with the full NLO and NNLO corrections for gluon fusion sub-process. We find that these NSV corrections are potentially large and enhance the pseudoscalar production cross-sections much more than the conventional SV or threshold logarithms. We also give numerical results for the NSV resummed results to $\overline{\text{NNLL}}$ accuracy by systematically matching to the FO NNLO cross-sections. We find that these NSV resummed predictions give large contributions to the cross-sections than what the SV resummation results do. We estimate the size of these corrections in terms of the resummed K-factors defined w.r.t. LO and find them to be as large as 3 at NNLO+ $\overline{\text{NNLL}}$ accuracy in the high mass region. We also estimate in our predictions the uncertainties due to the choice of various parton densities and those due to the unknown renormalization and factorization scales. We find that the conventional 7-point scale uncertainties do not get improvement after performing the NSV resummation, suggesting the requirement of including NSV contributions from other parton channels as well as beyond NSV contributions in the gluon fusion channel. However, for the pure μ_R variation, keeping μ_F fixed, we find that the scale uncertainties get reduced significantly to about 1.8% for $m_A = 700$ GeV and are much smaller than those of the SV resummed results ($\sim 6.4\%$).

ACKNOWLEDGMENTS

AB would like to thank Pooja Mukherjee and Surabhi Tiwari for useful discussions. AB is funded by the Department of Atomic Energy (DAE), India.

APPENDIX

Appendix A: NSV coefficient functions

In this section, we present our results of the NSV coefficient functions up to N³LO. Expanding the NSV cross-section, in powers of a_s , we obtain

$$\Delta_g^{A,NSV}(z, q^2) = \sum_{i=0}^{\infty} a_s^i \Delta_{g,i}^{A,NSV}(z, q^2). \quad (A1)$$

where

$$\begin{aligned} \Delta_{g,0}^{A,NSV} &= \delta(1-z), \\ \Delta_{g,1}^{A,NSV} &= \delta(1-z) \left[8C_A(1+\zeta_2) \right] + \mathcal{D}_1 \left[16C_A \right] - \left[16C_A \right] \log(1-z) + 8C_A, \\ \Delta_{g,2}^{A,NSV} &= \delta(1-z) \left[C_A^2 \left(+\frac{494}{3} - \frac{220\zeta_3}{3} - \frac{4\zeta_2^2}{5} + \frac{1112\zeta_2}{9} \right) \right. \\ &\quad \left. + C_A n_f \left(-\frac{82}{3} - \frac{80\zeta_2}{9} - \frac{8\zeta_3}{3} \right) + C_F n_f \left(-\frac{160}{3} + 12 \log \frac{\mu_R^2}{m_t^2} + 16\zeta_3 \right) \right] \\ &\quad + \mathcal{D}_0 \left[C_A^2 \left(-\frac{1616}{27} + \frac{176\zeta_2}{3} + 312\zeta_3 \right) + C_A n_f \left(\frac{224}{27} - \frac{32\zeta_2}{3} \right) \right] \\ &\quad + \mathcal{D}_1 \left[C_A^2 \left(+\frac{2224}{9} - 160\zeta_2 \right) - C_A n_f \left(\frac{160}{9} \right) \right] \\ &\quad + \mathcal{D}_2 \left[-C_A^2 \left(\frac{176}{3} \right) + C_A n_f \left(\frac{32}{3} \right) \right] + \mathcal{D}_3 \left[C_A^2 (128) \right] - \left[C_A^2 (128) \right] \log^3(1-z) \\ &\quad + \left[C_A^2 \left(\frac{920}{3} \right) - C_A n_f \left(\frac{32}{3} \right) \right] \log^2(1-z) + \left[C_A^2 \left(-\frac{2740}{9} + 160\zeta_2 \right) \right. \\ &\quad \left. + C_A n_f \left(\frac{244}{9} \right) \right] \log(1-z) + \left[C_A^2 \left(\frac{4340}{27} - \frac{608\zeta_2}{3} - 312\zeta_3 \right) - C_A n_f \left(\frac{392}{27} + \frac{32\zeta_2}{3} \right) \right], \\ \Delta_{g,3}^{A,NSV} &= \delta(1-z) \left[C_A^3 \left(\frac{114568}{27} - \frac{64096\zeta_2^3}{105} - 3932\zeta_3 + \frac{266155\zeta_2}{162} - \frac{4007\zeta_2^2}{10} \frac{7832\zeta_2\zeta_3}{3} + \frac{13216\zeta_3^2}{3} \right. \right. \\ &\quad \left. \left. - \frac{30316\zeta_5}{9} \right) + C_A^2 n_f \left(-\frac{113366}{81} - \frac{56453\zeta_2}{405} + \frac{21703\zeta_2^2}{135} + \frac{8840\zeta_3}{27} - \frac{2000C_A^2 n_f \zeta_2 \zeta_3}{3} + \frac{6952\zeta_5}{9} \right) \right. \\ &\quad + C_A n_f^2 \left(\frac{6914}{81} - \frac{7088C_A n_f^2 \zeta_2}{405} - \frac{2288C_A n_f^2 \zeta_2^2}{135} + \frac{688\zeta_3}{27} \right) + C_A C_F n_f \left(-1797 + 96 \log \frac{\mu_R^2}{m_t^2} \right. \\ &\quad \left. + \frac{176\zeta_2^2}{45} + \frac{1856\zeta_3}{3} + 192\zeta_2\zeta_3 + \frac{3872\zeta_5}{9} + 96 \log \frac{\mu_R^2}{m_t^2} \zeta_2 - \frac{4160\zeta_2}{9} \right) - 4C_J^{(2)} n_f \\ &\quad + C_F^2 n_f \left(\frac{457}{3} + 208\zeta_3 - 320\zeta_5 \right) + C_F n_f^2 \left(+\frac{1498}{9} - \frac{40\zeta_2}{9} - \frac{32\zeta_2^2}{45} - \frac{224\zeta_3}{3} \right) \Big] \\ &\quad + \mathcal{D}_5 \left[C_A^3 (512) \right] + \mathcal{D}_4 \left[-C_A^3 \left(\frac{7040}{9} \right) + C_A^3 n_f \left(\frac{1280}{9} \right) \right] + \mathcal{D}_3 \left[C_A^3 \left(\frac{86848C_A^3}{27} - 3584C_A^3 \zeta_2 \right) \right. \\ &\quad \left. + C_A^2 n_f \left(-\frac{10496}{27} + \frac{256}{27} \right) \right] + \mathcal{D}_2 \left[C_A^3 \left(-\frac{79936}{27} + \frac{11968\zeta_2}{3} + 11584\zeta_3 \right) \right. \\ &\quad \left. + C_A^2 n_f \left(\frac{16928}{27} - \frac{2176\zeta_2}{3} \right) + 32C_A C_F n_f - C_A n_f^2 \left(\frac{640}{27} \right) \right] + \mathcal{D}_1 \left[C_A^3 \left(\frac{414616}{81} \right. \right. \\ &\quad \left. \left. - \frac{13568\zeta_2}{3} - \frac{9856\zeta_2^2}{5} - \frac{22528\zeta_3}{3} \right) + C_A^2 n_f \left(-\frac{79760}{81} + \frac{6016\zeta_2}{9} + \frac{2944\zeta_3}{3} \right) \right. \\ &\quad \left. + C_A n_f^2 \left(\frac{1600}{81} - \frac{256\zeta_2}{9} \right) C_A C_F n_f \left(-1000 + 192 \log \frac{\mu_R^2}{m_t^2} + 384\zeta_3 \right) \right] + \mathcal{D}_0 \left[C_A^3 \left(-\frac{943114}{729} \right. \right. \end{aligned}$$

$$\begin{aligned}
& + \frac{17502\zeta_2}{81} + \frac{4048\zeta_2^2}{15} + \frac{210448\zeta_3}{27} - \frac{23200\zeta_2\zeta_3}{3} + 11904\zeta_5 \Big) + C_A^2 n_f \Big(\frac{173636C_A^2 n_f}{729} \\
& - \frac{41680C_A^2 n_f \zeta_2}{81} - \frac{544C_A^2 n_f \zeta_2^2}{15} - \frac{7600C_A^2 n_f \zeta_3}{9} \Big) + C_A n_f^2 \Big(-\frac{3712}{729} + \frac{640\zeta_2}{27} + \frac{320\zeta_3}{27} \Big) \\
& + C_A C_F n_f \Big(\frac{3422}{27} - 32\zeta_2 - \frac{64\zeta_2^2}{5} - \frac{608\zeta_3}{9} \Big) + \Big[-512C_A^3 \Big] \log^5(1-z) + \Big[\frac{22592C_A^3}{9} \\
& - \frac{1280C_A^2 n_f}{9} \Big] \log^4(1-z) + \Big[C_A^3 \Big(-\frac{138656}{27} + 3584\zeta_2 \Big) + \frac{6560C_A^2 n_f}{9} - \frac{256C_A n_f^2}{27} \Big] \log^3(1-z) \\
& + \Big[C_A^3 \Big(\frac{239744}{27} - \frac{34352\zeta_2}{3} - 11584\zeta_3 \Big) + C_A^2 n_f \Big(-\frac{34984}{27} + \frac{2180\zeta_2}{3} \Big) + C_A n_f^2 \Big(\frac{944}{27} \Big) \\
& - 32C_A C_F n_f \Big] \log^2(1-z) + \Big[C_A^3 \Big(-\frac{221824C_A^3}{27} + \frac{87520C_A^3 \zeta_2}{9} + \frac{9856C_A^3 \zeta_2^2}{5} + 23168C_A^3 \zeta_3 \Big) \\
& + C_A^2 n_f \Big(\frac{125860C_A^2 n_f}{81} - \frac{14504C_A^2 n_f \zeta_2}{9} - \frac{2992C_A^2 n_f \zeta_3}{3} \Big) + C_A n_f^2 \Big(-\frac{2608C_A n_f^2}{81} + \frac{256C_A n_f^2 \zeta_2}{9} \Big) \\
& + C_A C_F n_f \Big(1032C_A C_F n_f - 192C_A C_F n_f \log \frac{\mu_R^2}{m_t^2} - 384C_A C_F n_f \zeta_3 \Big) + n_f \Big(-4 + \frac{8\zeta_2}{3} \Big) \Big] \log(1-z) \\
& + \Big[C_A^3 \Big(\frac{2650990}{729} - \frac{489184\zeta_2}{81} - \frac{26272\zeta_2^2}{15} - \frac{330184\zeta_3}{27} + \frac{23200\zeta_2\zeta_3}{3} \\
& - 11904\zeta_5 \Big) + C_A^2 n_f \Big(-\frac{551267}{729} + \frac{80176\zeta_2}{81} + \frac{304\zeta_2^2}{5} + \frac{13736\zeta_3}{9} \Big) \\
& + C_A n_f^2 \Big(\frac{3136}{729} - \frac{304\zeta_2}{9} - \frac{320\zeta_3}{27} \Big) + C_A C_F n_f \Big(-\frac{1280}{3} + 96 \log \frac{\mu_R^2}{m_t^2} + 128\zeta_3 \Big) \\
& + n_f \Big(\frac{2653}{27} - \frac{40\zeta_2}{3} - \frac{32\zeta_2^2}{5} - \frac{616\zeta_3}{9} \Big) \Big]
\end{aligned} \tag{A2}$$

Appendix B: SV coefficients in soft collinear distribution

In this section, we present the explicit expressions for $\hat{\phi}_g^{SV,(i)}(\varepsilon)$ appearing in Eq. (37):

$$\begin{aligned}
\hat{\phi}_g^{SV,(1)}(\varepsilon) &= -\frac{3}{16}C_A\varepsilon^2\zeta_2^2 + \frac{8C_A}{\varepsilon^2} + \frac{7C_A\zeta_3}{3}\varepsilon - 3C_A\zeta_2, \\
\hat{\phi}_g^{SV,(2)}(\varepsilon) &= \varepsilon \left\{ \frac{3}{16}\beta_0 C_A \zeta_2^2 + \frac{11C_A^2\zeta_2^2}{80} - \frac{203}{6}C_A^2\zeta_2\zeta_3 + \frac{707C_A^2\zeta_2}{27} + \frac{2077C_A^2\zeta_3}{54} + \frac{43C_A^2\zeta_5}{2} \right. \\
&\quad - \frac{3644C_A^2}{243} - \frac{1}{40}C_A n_f \zeta_2^2 - \frac{98C_A n_f \zeta_2}{27} - \frac{155C_A n_f \zeta_3}{27} + \frac{488C_A n_f}{243} \Big\} + \left\{ 2C_A^2\zeta_2^2 \right. \\
&\quad - \frac{469C_A^2\zeta_2}{18} - \frac{88C_A^2\zeta_3}{3} + \frac{1214C_A^2}{81} + \frac{35C_A n_f \zeta_2}{9} + \frac{16C_A n_f \zeta_3}{3} - \frac{164C_A n_f}{81} - \frac{7\beta_0 C_A \zeta_3}{3} \Big\} \\
&\quad + \frac{1}{\varepsilon} \left\{ 6\beta_0 C_A \zeta_2 + \frac{11C_A^2\zeta_2}{3} + 14C_A^2\zeta_3 - \frac{404C_A^2}{27} - \frac{2C_A n_f \zeta_2}{3} + \frac{56C_A n_f}{27} \right\} \\
&\quad + \frac{1}{\varepsilon^2} \left\{ -4C_A^2\zeta_2 + \frac{134C_A^2}{9} - \frac{20C_A n_f}{9} \right\} - \frac{4\beta_0 C_A}{\varepsilon^3}, \\
\hat{\phi}_g^{SV,(3)}(\varepsilon) &= \frac{32\beta_0^2 C_A}{9\varepsilon^4} + \frac{1}{\varepsilon^3} \left\{ \frac{64}{9}\beta_0 C_A^2\zeta_2 - \frac{2144\beta_0 C_A^2}{81} + \frac{320\beta_0 C_A n_f}{81} - \frac{8\beta_1 C_A}{9} \right\} \\
&\quad + \frac{1}{\varepsilon^2} \left\{ -12\beta_0^2 C_A \zeta_2 - \frac{88}{9}\beta_0 C_A^2\zeta_2 - \frac{112}{3}\beta_0 C_A^2\zeta_3 + \frac{3232\beta_0 C_A^2}{81} + \frac{16}{9}\beta_0 C_A n_f \zeta_2 \right. \\
&\quad - \frac{448\beta_0 C_A n_f}{81} + \frac{352C_A^3\zeta_2^2}{45} - \frac{2144C_A^3\zeta_2}{81} + \frac{176C_A^3\zeta_3}{27} + \frac{980C_A^3}{27} + \frac{320}{81}C_A^2 n_f \zeta_2 \\
&\quad - \frac{224}{27}C_A^2 n_f \zeta_3 - \frac{1672C_A^2 n_f}{243} + \frac{64}{9}C_A C_f n_f \zeta_3 - \frac{220C_A C_f n_f}{27} - \frac{32C_A n_f^2}{243} \Big\} \\
&\quad + \frac{1}{\varepsilon} \left\{ -8\beta_0 C_A^2\zeta_2^2 + \frac{938}{9}\beta_0 C_A^2\zeta_2 + \frac{352}{3}\beta_0 C_A^2\zeta_3 - \frac{4856\beta_0 C_A^2}{81} - \frac{140}{9}\beta_0 C_A n_f \zeta_2 \right. \\
&\quad - \frac{64}{3}\beta_0 C_A n_f \zeta_3 + \frac{656\beta_0 C_A n_f}{81} + 3\beta_1 C_A \zeta_2 - \frac{352}{15}C_A^3\zeta_2^2 - \frac{176}{9}C_A^3\zeta_2\zeta_3 + \frac{12650C_A^3\zeta_2}{243} \\
&\quad + \frac{1316C_A^3\zeta_3}{9} - 64C_A^3\zeta_5 - \frac{136781C_A^3}{2187} + \frac{32}{5}C_A^2 n_f \zeta_2^2 - \frac{2828}{243}C_A^2 n_f \zeta_2 - \frac{728}{81}C_A^2 n_f \zeta_3 \\
&\quad + \frac{11842C_A^2 n_f}{2187} - \frac{32}{15}C_A C_f n_f \zeta_2^2 - \frac{4}{3}C_A C_f n_f \zeta_2 - \frac{304}{27}C_A C_f n_f \zeta_3 + \frac{1711C_A C_f n_f}{81} \\
&\quad + \frac{40}{81}C_A n_f^2 \zeta_2 - \frac{112}{81}C_A n_f^2 \zeta_3 + \frac{2080C_A n_f^2}{2187} \Big\} + \left\{ -\frac{11}{30}\beta_0 C_A^2\zeta_2^2 + \frac{812}{9}\beta_0 C_A^2\zeta_2\zeta_3 \right. \\
&\quad - \frac{5656}{81}\beta_0 C_A^2\zeta_2 - \frac{8308}{81}\beta_0 C_A^2\zeta_3 - \frac{172}{3}\beta_0 C_A^2\zeta_5 + \frac{29152\beta_0 C_A^2}{729} + \frac{1}{15}\beta_0 C_A n_f \zeta_2^2 \\
&\quad + \frac{1240}{81}\beta_0 C_A n_f \zeta_3 - \frac{3904\beta_0 C_A n_f}{729} + \frac{1}{16}\beta_1 C_A \varepsilon \zeta_2^2 - \frac{7\beta_1 C_A \zeta_3}{9} + \frac{152C_A^3\zeta_2^3}{189} + \frac{1964C_A^3\zeta_2^2}{27} \\
&\quad + \frac{11000}{27}C_A^3\zeta_2\zeta_3 - \frac{765127C_A^3\zeta_2}{1458} + \frac{536C_A^3\zeta_3}{9} - \frac{59648C_A^3\zeta_3}{81} - \frac{1430C_A^3\zeta_5}{9} + \frac{7135981C_A^3}{26244} \\
&\quad - \frac{532}{27}C_A^2 n_f \zeta_2^2 - \frac{1208}{27}C_A^2 n_f \zeta_2\zeta_3 + \frac{105059}{729}C_A^2 n_f \zeta_2 + \frac{45956}{243}C_A^2 n_f \zeta_3 + \frac{148}{9}C_A^2 n_f \zeta_5 \\
&\quad - \frac{716509C_A^2 n_f}{13122} + \frac{152}{45}C_A C_f n_f \zeta_2^2 - \frac{88}{3}C_A C_f n_f \zeta_2\zeta_3 + \frac{605}{18}C_A C_f n_f \zeta_2 + \frac{2536}{81}C_A C_f n_f \zeta_3 \\
&\quad + \frac{112}{9}C_A C_f n_f \zeta_5 - \frac{42727C_A C_f n_f}{972} + \frac{32}{27}C_A n_f^2 \zeta_2^2 - \frac{1996}{243}C_A n_f^2 \zeta_2 - \frac{2720}{243}C_A n_f^2 \zeta_3 \\
&\quad + \frac{11584C_A n_f^2}{6561} - \frac{1}{4}\beta_0^2 C_A \zeta_2^2 + \frac{784}{81}\beta_0 C_A n_f \zeta_2 \Big\}. \tag{B1}
\end{aligned}$$

Appendix C: Singular NSV coefficients in soft collinear distribution

In this section, we present the explicit expressions for the singular coefficients $\varphi_{s,g}^{NSV,(i)}(z,\varepsilon)$ appearing in Eq. (40):

$$\begin{aligned}
\varphi_{s,g}^{NSV,(1)}(z,\varepsilon) &= -\frac{8C_A}{\varepsilon}, \\
\varphi_{s,g}^{NSV,(2)}(z,\varepsilon) &= \frac{8\beta_0 C_A}{\varepsilon^2} + \frac{1}{\varepsilon} \left\{ C_A^2 \left(8\zeta_2 - \frac{268}{9} \right) + \frac{40C_A n_f}{9} + 16C_A^2 \log(1-z) \right\}, \\
\varphi_{s,g}^{NSV,(3)}(z,\varepsilon) &= -\frac{32\beta_0^2 C_A}{3\varepsilon^3} + \frac{1}{\varepsilon^2} \left\{ \frac{8\beta_1 C_A}{3} - \frac{8}{3}\beta_0 \left(C_A^2 \left(8\zeta_2 - \frac{268}{9} \right) + \frac{40C_A n_f}{9} \right. \right. \\
&\quad \left. \left. + 16C_A^2 \log(1-z) \right) \right\} + \frac{2}{3\varepsilon} \left\{ C_A^3 \left(-\frac{176\zeta_2^2}{5} + \frac{1072\zeta_2}{9} + \frac{56\zeta_3}{3} - 166 \right) \right. \\
&\quad \left. + \frac{80}{3} C_A^2 n_f T_f + C_A^2 n_f \left(-\frac{160\zeta_2}{9} + \frac{112\zeta_3}{3} + \frac{548}{27} \right) + 16C_A C_f n_f T_f \right. \\
&\quad \left. + C_A C_f n_f \left(\frac{86}{3} - 32\zeta_3 \right) + \frac{16C_A n_f^2}{27} + \log(1-z) \left(C_A^3 \left(\frac{2144}{9} - 64\zeta_2 \right) \right. \right. \\
&\quad \left. \left. - \frac{320C_A^2 n_f}{9} \right) \right\}. \tag{C1}
\end{aligned}$$

-
- [1] G. Aad *et al.* (ATLAS), Observation of a new particle in the search for the Standard Model Higgs boson with the ATLAS detector at the LHC, *Phys. Lett. B* **716**, 1 (2012), arXiv:1207.7214 [hep-ex].
 - [2] S. Chatrchyan *et al.* (CMS), Observation of a New Boson at a Mass of 125 GeV with the CMS Experiment at the LHC, *Phys. Lett. B* **716**, 30 (2012), arXiv:1207.7235 [hep-ex].
 - [3] P. W. Higgs, Broken symmetries, massless particles and gauge fields, *Phys. Lett.* **12**, 132 (1964).
 - [4] P. W. Higgs, Broken symmetries and the masses of gauge bosons, *Phys. Rev. Lett.* **13**, 508 (1964).
 - [5] P. W. Higgs, Spontaneous symmetry breakdown without massless bosons, *Phys. Rev.* **145**, 1156 (1966).
 - [6] F. Englert and R. Brout, Broken symmetry and the mass of gauge vector mesons, *Phys. Rev. Lett.* **13**, 321 (1964).
 - [7] G. S. Guralnik, C. R. Hagen, and T. W. B. Kibble, Global conservation laws and massless particles, *Phys. Rev. Lett.* **13**, 585 (1964).
 - [8] Combined coupling measurements of the Higgs-like boson with the ATLAS detector using up to 25 fb⁻¹ of proton-proton collision data (2013).
 - [9] G. Aad *et al.* (ATLAS), Combined measurements of Higgs boson production and decay using up to 80 fb⁻¹ of proton-proton collision data at $\sqrt{s} = 13$ TeV collected with the ATLAS experiment, *Phys. Rev. D* **101**, 012002 (2020), arXiv:1909.02845 [hep-ex].
 - [10] G. Aad, T. Abajyan, B. Abbott, J. Abdallah, S. Abdel Khalek, O. Abdinov, R. Aben, B. Abi, M. Abolins, O. AbouZeid, and et al., Evidence for the spin-0 nature of the higgs boson using atlas data, *Physics Letters B* **726**, 120–144 (2013).
 - [11] V. Khachatryan *et al.* (CMS), Constraints on the spin-parity and anomalous HVV couplings of the Higgs boson in proton collisions at 7 and 8 TeV, *Phys. Rev. D* **92**, 012004 (2015), arXiv:1411.3441 [hep-ex].
 - [12] R. V. Harlander and W. B. Kilgore, Production of a pseudo-scalar higgs boson at hadron colliders at next-to-next-to-leading order, *Journal of High Energy Physics* **2002**, 017–017 (2002).
 - [13] C. Anastasiou and K. Melnikov, Pseudoscalar Higgs boson production at hadron colliders in NNLO QCD, *Phys. Rev. D* **67**, 037501 (2003), arXiv:hep-ph/0208115.
 - [14] V. Ravindran, J. Smith, and W. van Neerven, Nnlo corrections to the total cross section for higgs boson production in hadron–hadron collisions, *Nuclear Physics B* **665**, 325–366 (2003).
 - [15] C. Anastasiou and K. Melnikov, Higgs boson production at hadron colliders in nnlo qcd, *Nuclear Physics B* **646**, 220–256 (2002).
 - [16] R. V. Harlander and W. B. Kilgore, Next-to-next-to-leading order Higgs production at hadron colliders, *Phys. Rev. Lett.* **88**, 201801 (2002), arXiv:hep-ph/0201206.
 - [17] R. V. Harlander and K. J. Ozeren, Top mass effects in Higgs production at next-to-next-to-leading order QCD: Virtual corrections, *Phys. Lett. B* **679**, 467 (2009), arXiv:0907.2997 [hep-ph].
 - [18] R. V. Harlander and K. J. Ozeren, Finite top mass effects for hadronic Higgs production at next-to-next-to-leading order, *JHEP* **11**, 088, arXiv:0909.3420 [hep-ph].
 - [19] A. Pak, M. Rogal, and M. Steinhauser, Finite top quark mass effects in NNLO Higgs boson production at LHC, *JHEP* **02**, 025, arXiv:0911.4662 [hep-ph].
 - [20] R. V. Harlander and W. B. Kilgore, Production of a pseudoscalar Higgs boson at hadron colliders at next-to-next-to leading order, *JHEP* **10**, 017, arXiv:hep-ph/0208096.
 - [21] C. Anastasiou, C. Duhr, F. Dulat, E. Furlan, T. Gehrmann, F. Herzog, and B. Mistlberger, Higgs boson gluon–fusion production at threshold in n³lo qcd, *Physics Letters B* **737**, 325 (2014).
 - [22] C. Anastasiou, C. Duhr, F. Dulat, E. Furlan, T. Gehrmann, F. Herzog, A. Lazopoulos, and B. Mistlberger, High precision determination of the gluon fusion Higgs boson cross-section at the LHC, *JHEP* **05**, 058, arXiv:1602.00695 [hep-ph].
 - [23] C. Duhr and B. Mistlberger, Lepton-pair production at hadron colliders at N³LO in QCD (2021), arXiv:2111.10379 [hep-ph].
 - [24] T. Ahmed, M. Kumar, P. Mathews, N. Rana, and V. Ravindran, Pseudo-scalar Higgs boson production at threshold N³ LO and N³ LL QCD, *Eur. Phys. J. C* **76**, 355 (2016), 1510.02235.
 - [25] T. Ahmed, M. Bonvini, M. C. Kumar, P. Mathews, N. Rana, V. Ravindran, and L. Rottoli, Pseudo-scalar Higgs boson production at N³LO_A + N³LL', *Eur. Phys. J. C* **76**, 663 (2016), arXiv:1606.00837 [hep-ph].
 - [26] S. Catani, D. de Florian, M. Grazzini, and P. Nason, Soft gluon resummation for Higgs boson production at hadron colliders, *JHEP* **07**, 028, arXiv:hep-ph/0306211.
 - [27] S. Moch and A. Vogt, Higher-order soft corrections to lepton pair and higgs boson production, *Physics Letters B* **631**, 48–57 (2005).
 - [28] E. Laenen and L. Magnea, Threshold resummation for electroweak annihilation from dis data, *Physics Letters B* **632**, 270–276 (2006).
 - [29] V. Ravindran, On sudakov and soft resummations in qcd, *Nuclear Physics B* **746**, 58–76 (2006).
 - [30] V. Ravindran, Higher-order threshold effects to inclusive processes in QCD, *Nucl. Phys. B* **752**, 173 (2006), arXiv:hep-ph/0603041.
 - [31] A. Idilbi, X.-d. Ji, J.-P. Ma, and F. Yuan, Threshold resummation for Higgs production in effective field theory, *Phys. Rev. D* **73**, 077501 (2006), arXiv:hep-ph/0509294.
 - [32] V. Ahrens, T. Becher, M. Neubert, and L. L. Yang, Renormalization-group improved prediction for higgs production at hadron colliders, *The European Physical Journal C* **62**, 333–353 (2009).

- [33] D. de Florian and M. Grazzini, Higgs production through gluon fusion: Updated cross sections at the tevatron and the lhc, *Physics Letters B* **674**, 291–294 (2009).
- [34] T. Schmidt and M. Spira, Higgs Boson Production via Gluon Fusion: Soft-Gluon Resummation including Mass Effects, *Phys. Rev. D* **93**, 014022 (2016), arXiv:1509.00195 [hep-ph].
- [35] C. Anastasiou, C. Duhr, F. Dulat, F. Herzog, and B. Mistlberger, Higgs Boson Gluon-Fusion Production in QCD at Three Loops, *Phys. Rev. Lett.* **114**, 212001 (2015), arXiv:1503.06056 [hep-ph].
- [36] M. Bonvini and S. Marzani, Resummed Higgs cross section at N^3LL , *JHEP* **09**, 007, arXiv:1405.3654 [hep-ph].
- [37] M. Bonvini, S. Marzani, C. Muselli, and L. Rottoli, On the Higgs cross section at N^3LO+N^3LL and its uncertainty, *JHEP* **08**, 105, arXiv:1603.08000 [hep-ph].
- [38] T. Ahmed, T. Gehrmann, P. Mathews, N. Rana, and V. Ravindran, Pseudo-scalar Form Factors at Three Loops in QCD, *JHEP* **11**, 169, arXiv:1510.01715 [hep-ph].
- [39] S. Moch and A. Vogt, Higher-order soft corrections to lepton pair and Higgs boson production, *Phys. Lett. B* **631**, 48 (2005), arXiv:hep-ph/0508265.
- [40] D. de Florian and J. Mazzitelli, A next-to-next-to-leading order calculation of soft-virtual cross sections, *JHEP* **12**, 088, arXiv:1209.0673 [hep-ph].
- [41] T. Ahmed, M. Mahakhud, N. Rana, and V. Ravindran, Drell-Yan Production at Threshold to Third Order in QCD, *Phys. Rev. Lett.* **113**, 112002 (2014), arXiv:1404.0366 [hep-ph].
- [42] S. Catani, L. Cieri, D. de Florian, G. Ferrera, and M. Grazzini, Threshold resummation at N^3LL accuracy and soft-virtual cross sections at N^3LO , *Nucl. Phys. B* **888**, 75 (2014), arXiv:1405.4827 [hep-ph].
- [43] T. Ahmed, N. Rana, and V. Ravindran, Higgs boson production through $b\bar{b}$ annihilation at threshold in N^3LO QCD, *JHEP* **10**, 139, arXiv:1408.0787 [hep-ph].
- [44] M. Kumar, M. Mandal, and V. Ravindran, Associated production of Higgs boson with vector boson at threshold N^3LO in QCD, *JHEP* **03**, 037, arXiv:1412.3357 [hep-ph].
- [45] Y. Li, A. von Manteuffel, R. M. Schabinger, and H. X. Zhu, N^3LO Higgs boson and Drell-Yan production at threshold: The one-loop two-emission contribution, *Phys. Rev. D* **90**, 053006 (2014), arXiv:1404.5839 [hep-ph].
- [46] G. Sterman, Summation of large corrections to short-distance hadronic cross sections, *Nuclear Physics B* **281**, 310 (1987).
- [47] S. Catani and L. Trentadue, Resummation of the qcd perturbative series for hard processes, *Nuclear Physics B* **327**, 323 (1989).
- [48] S. Catani, M. L. Mangano, P. Nason, and L. Trentadue, The resummation of soft gluons in hadronic collisions, *Nuclear Physics B* **478**, 273 (1996).
- [49] S. Moch, J. Vermaseren, and A. Vogt, Higher-order corrections in threshold resummation, *Nucl. Phys. B* **726**, 317 (2005), arXiv:hep-ph/0506288.
- [50] M. Bonvini, S. Forte, and G. Ridolfi, The Threshold region for Higgs production in gluon fusion, *Phys. Rev. Lett.* **109**, 102002 (2012), arXiv:1204.5473 [hep-ph].
- [51] M. Bonvini and S. Marzani, Resummed Higgs cross section at N^3LL , *JHEP* **09**, 007, arXiv:1405.3654 [hep-ph].
- [52] M. Bonvini and L. Rottoli, Three loop soft function for N^3LL' gluon fusion Higgs production in soft-collinear effective theory, *Phys. Rev. D* **91**, 051301 (2015), arXiv:1412.3791 [hep-ph].
- [53] M. Bonvini, A. S. Papanastasiou, and F. J. Tackmann, Matched predictions for the $b\bar{b}H$ cross section at the 13 TeV LHC, *JHEP* **10**, 053, arXiv:1605.01733 [hep-ph].
- [54] A. H. Ajjath, A. Chakraborty, G. Das, P. Mukherjee, and V. Ravindran, Resummed prediction for Higgs boson production through $b\bar{b}$ annihilation at N^3LL , *JHEP* **11**, 006, arXiv:1905.03771 [hep-ph].
- [55] M. Bonvini, Threshold resummation for Drell-Yan production: Theory and phenomenology, *PoS DIS2010*, 100 (2010), arXiv:1006.5918 [hep-ph].
- [56] M. Bonvini, *Resummation of soft and hard gluon radiation in perturbative QCD*, Ph.D. thesis, Genoa U. (2012), arXiv:1212.0480 [hep-ph].
- [57] A. H. Ajjath, G. Das, M. C. Kumar, P. Mukherjee, V. Ravindran, and K. Samanta, Resummed Drell-Yan cross-section at N^3LL , *JHEP* **10**, 153, arXiv:2001.11377 [hep-ph].
- [58] E. Laenen, L. Magnea, and G. Stavenga, On next-to-eikonal corrections to threshold resummation for the Drell-Yan and DIS cross sections, *Phys. Lett. B* **669**, 173 (2008), arXiv:0807.4412 [hep-ph].
- [59] E. Laenen, L. Magnea, G. Stavenga, and C. D. White, Next-to-Eikonal Corrections to Soft Gluon Radiation: A Diagrammatic Approach, *JHEP* **01**, 141, arXiv:1010.1860 [hep-ph].
- [60] D. Bonocore, E. Laenen, L. Magnea, L. Vernazza, and C. D. White, The method of regions and next-to-soft corrections in Drell-Yan production, *Phys. Lett. B* **742**, 375 (2015), arXiv:1410.6406 [hep-ph].
- [61] D. Bonocore, E. Laenen, L. Magnea, S. Melville, L. Vernazza, and C. D. White, A factorization approach to next-to-leading-power threshold logarithms, *JHEP* **06**, 008, arXiv:1503.05156 [hep-ph].
- [62] D. Bonocore, E. Laenen, L. Magnea, L. Vernazza, and C. D. White, Non-abelian factorisation for next-to-leading-power threshold logarithms, *JHEP* **12**, 121, arXiv:1610.06842 [hep-ph].
- [63] V. Del Duca, E. Laenen, L. Magnea, L. Vernazza, and C. D. White, Universality of next-to-leading power threshold effects for colourless final states in hadronic collisions, *JHEP* **11**, 057, arXiv:1706.04018 [hep-ph].
- [64] N. Bahjat-Abbas, D. Bonocore, J. Sinninghe Damsté, E. Laenen, L. Magnea, L. Vernazza, and C. D. White, Diagrammatic resummation of leading-logarithmic threshold effects at next-to-leading power, *JHEP* **11**, 002, arXiv:1905.13710 [hep-ph].
- [65] S. Moch and A. Vogt, On non-singlet physical evolution kernels and large-x coefficient functions in perturbative QCD, *JHEP* **11**, 099, arXiv:0909.2124 [hep-ph].

- [66] M. Beneke, A. Broggio, M. Garny, S. Jaskiewicz, R. Szafron, L. Vernazza, and J. Wang, Leading-logarithmic threshold resummation of the Drell-Yan process at next-to-leading power, *JHEP* **03**, 043, arXiv:1809.10631 [hep-ph].
- [67] M. Beneke, M. Garny, S. Jaskiewicz, R. Szafron, L. Vernazza, and J. Wang, Leading-logarithmic threshold resummation of Higgs production in gluon fusion at next-to-leading power, *JHEP* **01**, 094, arXiv:1910.12685 [hep-ph].
- [68] M. Beneke, A. Broggio, S. Jaskiewicz, and L. Vernazza, Threshold factorization of the Drell-Yan process at next-to-leading power, *JHEP* **07**, 078, arXiv:1912.01585 [hep-ph].
- [69] A. H. Ajjath, P. Mukherjee, and V. Ravindran, On next to soft corrections to Drell-Yan and Higgs Boson productions (2020), arXiv:2006.06726 [hep-ph].
- [70] M. van Beekveld, E. Laenen, J. Sinninghe Damsté, and L. Vernazza, Next-to-leading power threshold corrections for finite order and resummed colour-singlet cross sections, *JHEP* **05**, 114, arXiv:2101.07270 [hep-ph].
- [71] V. Ravindran, Higher-order threshold effects to inclusive processes in qcd, *Nuclear Physics B* **752**, 173–196 (2006).
- [72] K. Chetyrkin, B. Kniesl, M. Steinhauser, and W. Bardeen, Effective qcd interactions of cp-odd higgs bosons at three loops, *Nuclear Physics B* **535**, 3–18 (1998).
- [73] S. L. Adler, Axial-vector vertex in spinor electrodynamics, *Phys. Rev.* **177**, 2426 (1969).
- [74] O. Tarasov, A. Vladimirov, and A. Zharkov, The gell-mann-low function of qcd in the three-loop approximation, *Physics Letters B* **93**, 429 (1980).
- [75] A. Bhattacharya, M. Mahakhud, P. Mathews, and V. Ravindran, Two loop QCD amplitudes for di-pseudo scalar production in gluon fusion, *JHEP* **02**, 121, arXiv:1909.08993 [hep-ph].
- [76] V. Ravindran, J. Smith, and W. van Neerven, Two-loop corrections to Higgs boson production, *Nucl. Phys. B* **704**, 332 (2005), arXiv:hep-ph/0408315.
- [77] V. Sudakov, Vertex parts at very high-energies in quantum electrodynamics, *Sov. Phys. JETP* **3**, 65 (1956).
- [78] A. H. Mueller, On the Asymptotic Behavior of the Sudakov Form-factor, *Phys. Rev. D* **20**, 2037 (1979).
- [79] J. C. Collins, Algorithm to Compute Corrections to the Sudakov Form-factor, *Phys. Rev. D* **22**, 1478 (1980).
- [80] A. Sen, Asymptotic Behavior of the Sudakov Form-Factor in QCD, *Phys. Rev. D* **24**, 3281 (1981).
- [81] L. Magnea and G. F. Sterman, Analytic continuation of the Sudakov form-factor in QCD, *Phys. Rev. D* **42**, 4222 (1990).
- [82] V. Ravindran, On Sudakov and soft resummations in QCD, *Nucl. Phys. B* **746**, 58 (2006), arXiv:hep-ph/0512249.
- [83] S. Moch, J. Vermaseren, and A. Vogt, Three-loop results for quark and gluon form factors, *Physics Letters B* **625**, 245–252 (2005).
- [84] S. Moch, J. Vermaseren, and A. Vogt, The Three loop splitting functions in QCD: The Nonsinglet case, *Nucl. Phys. B* **688**, 101 (2004), arXiv:hep-ph/0403192.
- [85] A. Vogt, S. Moch, and J. Vermaseren, The Three-loop splitting functions in QCD: The Singlet case, *Nucl. Phys. B* **691**, 129 (2004), arXiv:hep-ph/0404111.
- [86] A. Vogt, Next-to-next-to-leading logarithmic threshold resummation for deep inelastic scattering and the Drell-Yan process, *Phys. Lett. B* **497**, 228 (2001), arXiv:hep-ph/0010146.
- [87] V. Ravindran, J. Smith, and W. L. van Neerven, NNLO corrections to the total cross-section for Higgs boson production in hadron hadron collisions, *Nucl. Phys. B* **665**, 325 (2003), arXiv:hep-ph/0302135.
- [88] C. Anastasiou, C. Duhr, F. Dulat, E. Furlan, T. Gehrmann, F. Herzog, and B. Mistlberger, Higgs boson gluon-fusion production at threshold in N^3 LO QCD, *Phys. Lett. B* **737**, 325 (2014), arXiv:1403.4616 [hep-ph].
- [89] S. Moch, J. Vermaseren, and A. Vogt, Higher-order corrections in threshold resummation, *Nuclear Physics B* **726**, 317–335 (2005).
- [90] R. D. Ball, M. Bonvini, S. Forte, S. Marzani, and G. Ridolfi, Higgs production in gluon fusion beyond nnlo, *Nuclear Physics B* **874**, 746–772 (2013).
- [91] M. Bonvini, R. D. Ball, S. Forte, S. Marzani, and G. Ridolfi, Updated Higgs cross section at approximate N^3 LO, *J. Phys. G* **41**, 095002 (2014), arXiv:1404.3204 [hep-ph].
- [92] M. Bonvini, S. Marzani, C. Muselli, and L. Rottoli, On the Higgs cross section at N^3 LO+ N^3 LL and its uncertainty, *JHEP* **08**, 105, arXiv:1603.08000 [hep-ph].
- [93] M. Bonvini and S. Marzani, Double resummation for Higgs production, *Phys. Rev. Lett.* **120**, 202003 (2018), arXiv:1802.07758 [hep-ph].
- [94] M. Bonvini, Small- x phenomenology at the LHC and beyond: HELL 3.0 and the case of the Higgs cross section, *Eur. Phys. J. C* **78**, 834 (2018), arXiv:1805.08785 [hep-ph].